N64-16766
CODE-1
CR-55849

79p.

[redacted]

NASA CR 55849

OTS PRICE

XEROX $ 7.60 ph
MICROFILM $ 2.57 mf.

ELECTRO-OPTICAL SYSTEMS, INC. Pasadena, California

PRELIMINARY DRAFT

~~f~~Final Report~~, for~~ 25 June 1962 to 25 February 1963

EVALUATION OF REGENERATIVE FUEL CELL

Prepared for

National Aeronautics and Space Administration
Western Operations Office
150 Pico Boulevard
Santa Monica, California

OTS

2 (NASA Contract NAS 7-181)

OTS: $7.60ph, $2.57mf

(NASA CR-55849; EOS-~~Report~~ 3310-Final) 12 July 1963 79p

Prepared by

J. J. Rowlette

J. J. Rowlette
Project Supervisor

Approved by

B. M. Wilner

B. M. Wilner, Manager
Chemical and Fluid
Systems Department

Approved by

for B. M. Wilner

J. Neustein, Manager
Advanced Power Systems
Division

ELECTRO-OPTICAL SYSTEMS, INC., PASADENA, CALIFORNIA

0845461

TABLE OF CONTENTS

LIST OF ILLUSTRATIONS

LIST OF ILLUSTRATIONS

LIST OF TABLES

1. SUMMARY

Regenerative hydrogen-oxygen fuel cells have the potential of achieving very high energy storage to weight ratios. However, for minimum weight of the energy conversion-storage system, it soon becomes evident that a premium is placed on cell efficiency. For this reason, the principal aim of this program was to develop cells with higher efficiencies while retaining the potential for high energy to weight ratios.

One approach to the problem is to develop a hybrid fuel cell that will retain in part the lightweight characteristics of the hydrogen-oxygen fuel cell and has far less electrode polarization associated with it. For this reason, a significant part of the program was devoted to work on hydrogen-silver oxide "fuel cells". When charging or discharging on the lower plateau (i.e., the Ag-Ag_2O plateau) of a silver electrode very high charge-discharge efficiencies have been achieved. When charges at 10 ma/cm^2 are discharged at 40, the voltage efficiency is 87 percent. Methods were sought to overcome some of the major disadvantages of the silver oxide electrode. Generally, it has been possible to charge only a small fraction of the theoretical amount on the lower plateau and discharge only a small amount on the upper plateau, thereby resulting in a significant energy loss. These limitations of the silver oxide electrode are believed to be connected with the high resistivity of Ag_2O. Resistivities of several doped silver oxides were measured and extensive testing was then performed on electrodes made from the two best of these and compared with undoped silver oxide electrodes. Resistivity values for all electrodes tested are given in Table VIII. Small improvements were noted in both capacity and polarization characteristics. In connection with the hydrogen-silver oxide concept,

hydrogen storage in palladium and in Raney nickel was evaluated for non-pressure storage of the hydrogen. It was concluded that for palladium, this approach is feasible, but for Raney nickel, it was not feasible with the present design.

An evaluation was made of a battery fuel cell based on the hydrogen-silver oxide reaction. Preliminary design of a battery based on the experimental results indicated only a small improvement in energy to weight ratio over other existing cells using silver oxide electrodes. Since the hydrogen-silver oxide hybrid fuel cell does not offer the potential for high energy to weight ratios, efforts for developing this cell further were limited.

It appears that the quantity of hydrogen stored was limited by the capacity of the palladium (i.e., the amount of hydrogen that forms a non-stoichoimetric compound of the composition $PdH_{0.55-0.60}$) that has been reported in the literature. The storage of hydrogen in palladium does not appear practical due to the high weight of palladium required.

Another major part of the program was concerned with investigations of the hydrogen-oxygen fuel cell. Electrode studies were carried out for the purpose of improving cell efficiencies and increasing power densities. These studies resulted in improvements in power densities at a given temperature of approximately a factor of five over performance available at the start of the program. For example, the maximum power density for a room temperature cell was less than 20 mw/cm^2 at the beginning of the program and increased to 90 mw/cm^2 at the end.

Experiments relating to other aspects of rechargeable hydrogen-oxygen fuel cells were also carried out. Since cell capacity is determined by the amount of electrolyte storage, methods of storing electrolyte in regions other than between the electrodes were examined. Significant improvements in capacity were demonstrated. A cell with a normal capacity of 3.5 amp-hours was increased to 9.2 amp-hours. From Fig. 11, it would appear that the cell should operate over an electrolyte concentration range of 35 percent KOH to the saturation point (about 54 percent at room temperature) for the complete charge-discharge cycle. Since the electrolyte bed serves the function of separating the gaseous reactants, measurements were made of gas diffusion rates through the electrolyte and methods are suggested for decreasing the gas permeability, thereby improving charge retention capabilities. It was found, for example, that for a completely discharged cell at room temperature and 100 psig that gas diffusion rates through the asbestos corresponded to approximately 0.9 ma/cm^2.

2. CONSTRUCTION OF EXPERIMENTAL CELLS

The design of the experimental fuel cell was such that it could be used either as a hydrogen-silver oxide cell or a hydrogen-oxygen cell. Figure 1 shows the arrangement when used as a hydrogen-oxygen cell. The silver oxide subassembly can be replaced by an oxygen subassembly which is identical to the one for hydrogen except that the storage tank has only half the capacity of the hydrogen tank and has no pressure transducer. The hydrogen-oxygen arrangement is shown in Figure 2.

It can be seen in Figures 1 and 2 that the fuel cell assembly contains two reference electrodes for measuring individual electrode potentials. Contact to these reference electrodes is made by Teflon insulated probes. The work performed on the present program did not require the use of micro electrodes as very rapid response times were not important. A 3 mm separation was made between the reference and working electrodes. Other investigators have attributed instability of their reference electrodes to high currents flowing in their immediate vicinity (Ref. 1). This difficulty has been overcome in the present design by not having working and reference electrodes opposite one another.

The working electrodes described in Sections 4.1 and 5.1 are annular rings with 3.968 cm outside diameter and 1.728 cm inside diameter. These dimensions are such that the working electrode area is exactly 10 cm^2 so that conversion from current to current density can readily be made.

The hydrogen and oxygen storage cylinders are stainless steel, and the fuel cell body is monel. The O-rings are silicone rubber.

In some cases, the electrolyte was made from boiled distilled water stored in glass. The boiling was done in order to reduce the carbon dioxide concentration which is originally far above the equilibrium value. The pH rises to 7.0 after boiling. In other cases, deionized water was used, since it has a very low CO_2 concentration. Potassium hydroxide solutions of 10, 35, and 55 percent were made up in advance and stored in polyethylene. The solutions were protected from the air by KOH pellets and color-indicating silica gel. The matrix holding the electrolyte was a commercial grade asbestos, which was washed before use to extract chloride ion which is present in the original material.

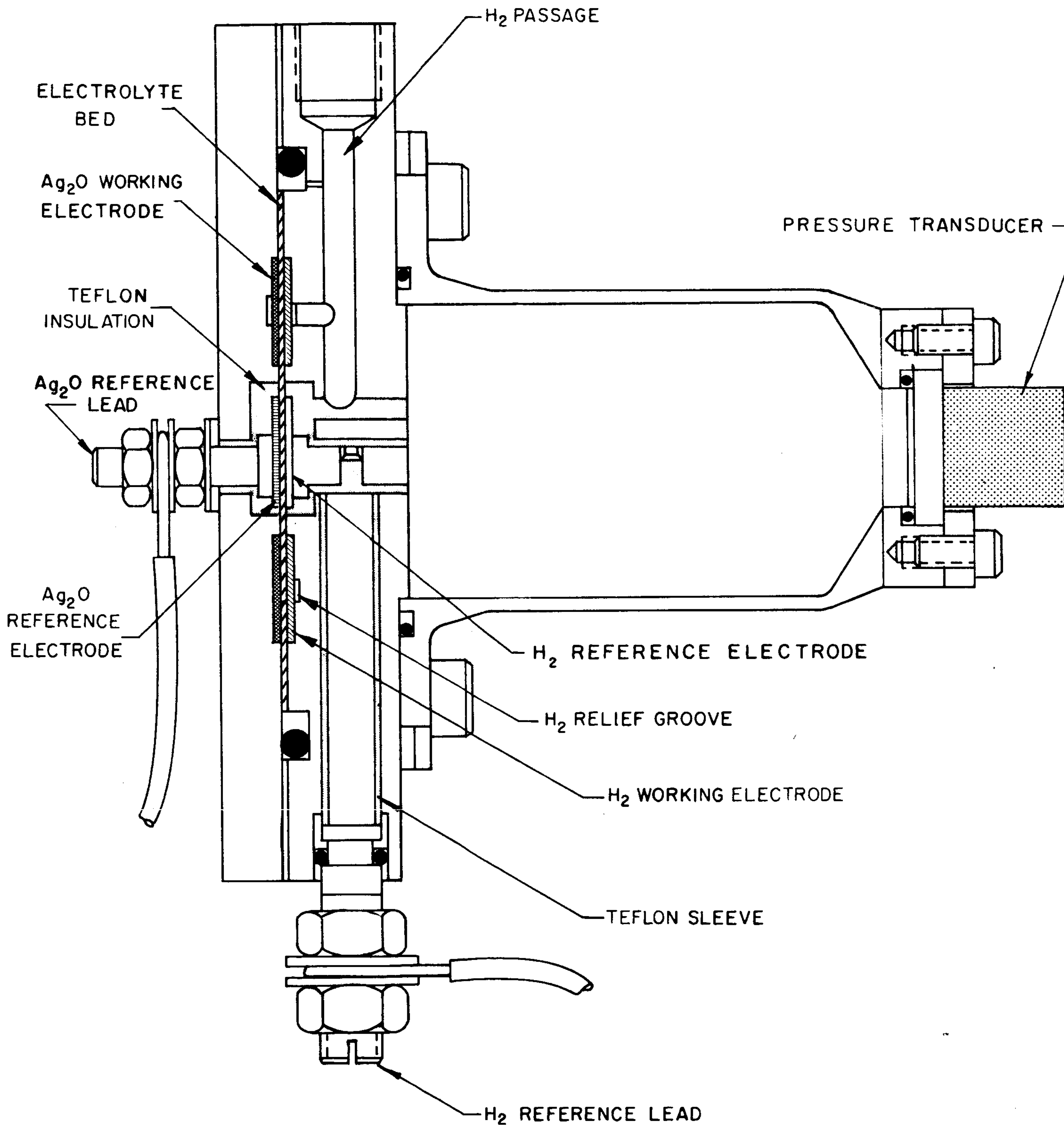

FIG. 1 HYDROGEN-SILVER OXIDE CELL

3510-Final

7365771

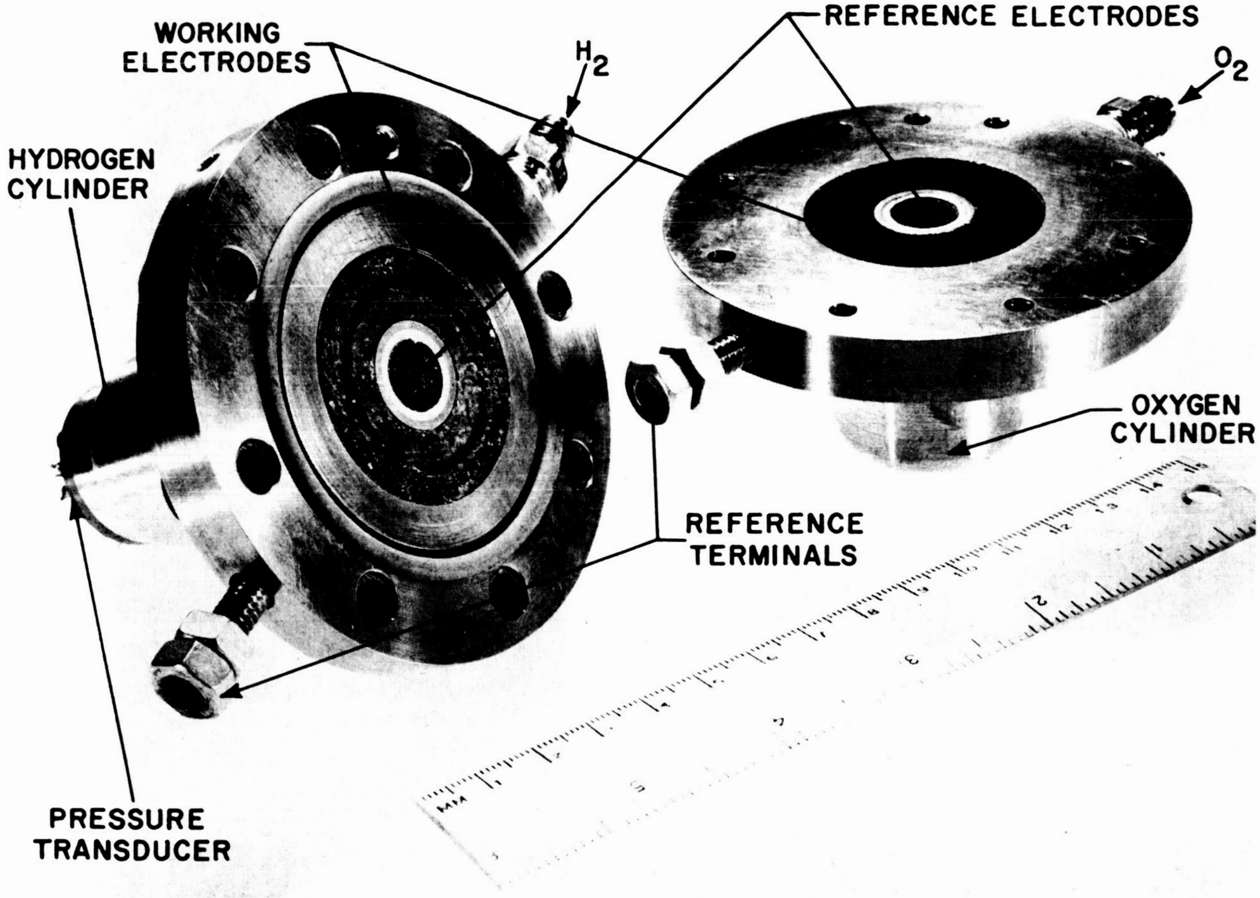

FIG. 2 FUEL CELL WITH REFERENCE ELECTRODES

3. INSTRUMENTATION

The instrumentation was designed for the purpose of measuring and recording individual electrode potentials of an operating cell in addition to temperature, pressure, and current. A pressure transducer was calibrated and built into the hydrogen storage cylinder (Figure 1). Temperature measurements were made with a chromel-alumel thermocouple with a room temperature reference junction. Current was inferred by measuring the voltage drop across a precision (1 percent) 0.1 ohm resistor.

A constant current power supply and cycler unit was built to obtain electrode polarizations as a function of current density. A schematic diagram of this unit is shown in Figure 3. Its purpose was to measure the fuel cell potential, the individual electrode polarizations, temperature, and pressure while the current was varied automatically on both charge and discharge. Beginning with an initial open circuit, the cycler went through a charge cycle at 100 ma, 200 ma, 400 ma, 600 ma, etc., to 2 amps, in that order. It then went to open circuit, through a discharge cycle at the same current settings as for the charge cycle, and returned to open circuit. At each setting, the power supply maintained constant current (although not exactly the nominal values mentioned above), and the time spent at each position could be set for 1, 2, 3, 4, 6, and 12 minutes. Three minute settings were used in all cases.

The various functions were monitored by a Brown-Honeywell eight-channel recorder. A channel selector panel was built so that each channel could be scaled individually to the recorder, by means of a potentiometer. The temperature channel was unscaled and therefore read from 0 to 20 mv, the sensitivity of the recorder. The pressure channel was scaled 0-40 mv, in some cases, allowing pressures to 350 psi to be recorded. At other times it was unscaled. The channel measuring hydrogen electrode polarization was originally scaled 0 - 0.2 volt, but was later changed to 0 - 0.4 volt. The current channel was scaled 0 - 0.2 volt, which implies 0.2 amp, and all other channels were scaled 0 - 2 volts. A reference voltage supply unit made by John Fluke Manufacturing Company was used as the primary standard for all voltage measurements above 1.02 volts, the potential of the standard cell.

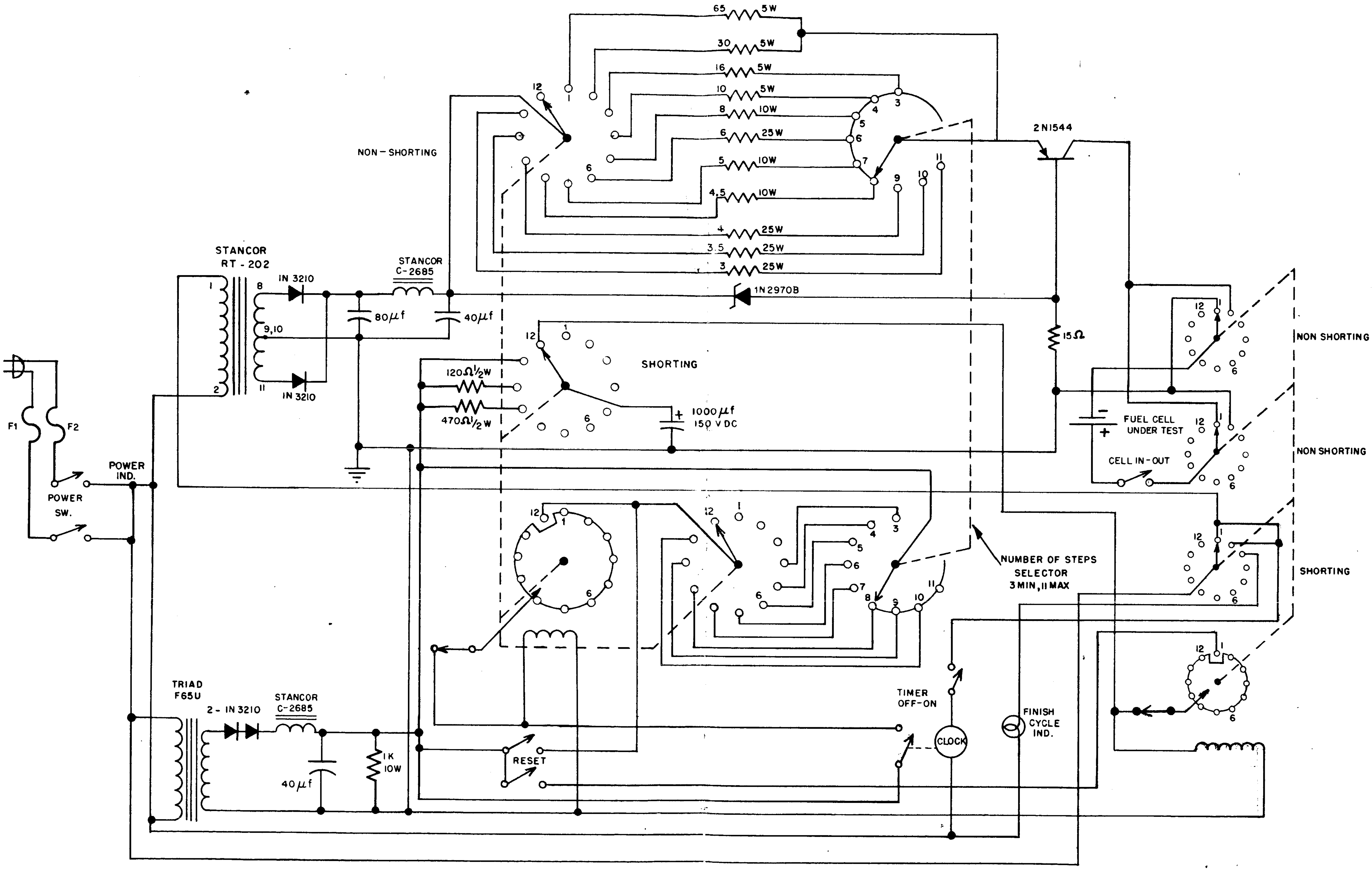

FIG. 3 CIRCUIT DIAGRAM OF CONSTANT CURRENT SUPPLY-CYCLER

4. HYDROGEN-OXYGEN CELLS

The part of the program devoted to research on hydrogen-oxygen cells was concerned with increasing cell performance, increasing the cell storage capacity, and measuring charge retention abilities and over-all cycle efficiency. By cell performance, it is meant voltage versus current density characteristics. Cell performance is determined very largely by the nature of the electrodes, but other factors can have a significant effect. These other factors are included under the general heading of electrode studies.

All studies of hydrogen-oxygen cells were made with catalyzed porous nickel electrodes. In all cases the electrolyte was contained in an asbestos matrix of about 0.08 cm thickness. The asbestos contains an organic binder that is quite stable in the fuel cell environment and adds a high degree of cohesion to the fibers. The resistivity of the electrolyte in the asbestos, as measured by a conductance bridge, is about 36 ohm-cm.

4.1 Electrode Fabrication

A major improvement in polarization characteristics for hydrogen-oxygen cells was achieved early in the program. A comparison between the old and new processes is shown in Fig. 4. Hydrogen and oxygen electrodes were made in this laboratory in the past by immersing porous nickel electrodes in a hot solution of chloroplatinic acid until the solution turned green or for a length of time considered sufficient to reduce all the platinum. But this process plated only a thin surface layer. The new plating process is accomplished by slowly drawing the solution through the electrode material, using the suction from a water aspirator. The electrode is placed in a Buchner funnel for this purpose.

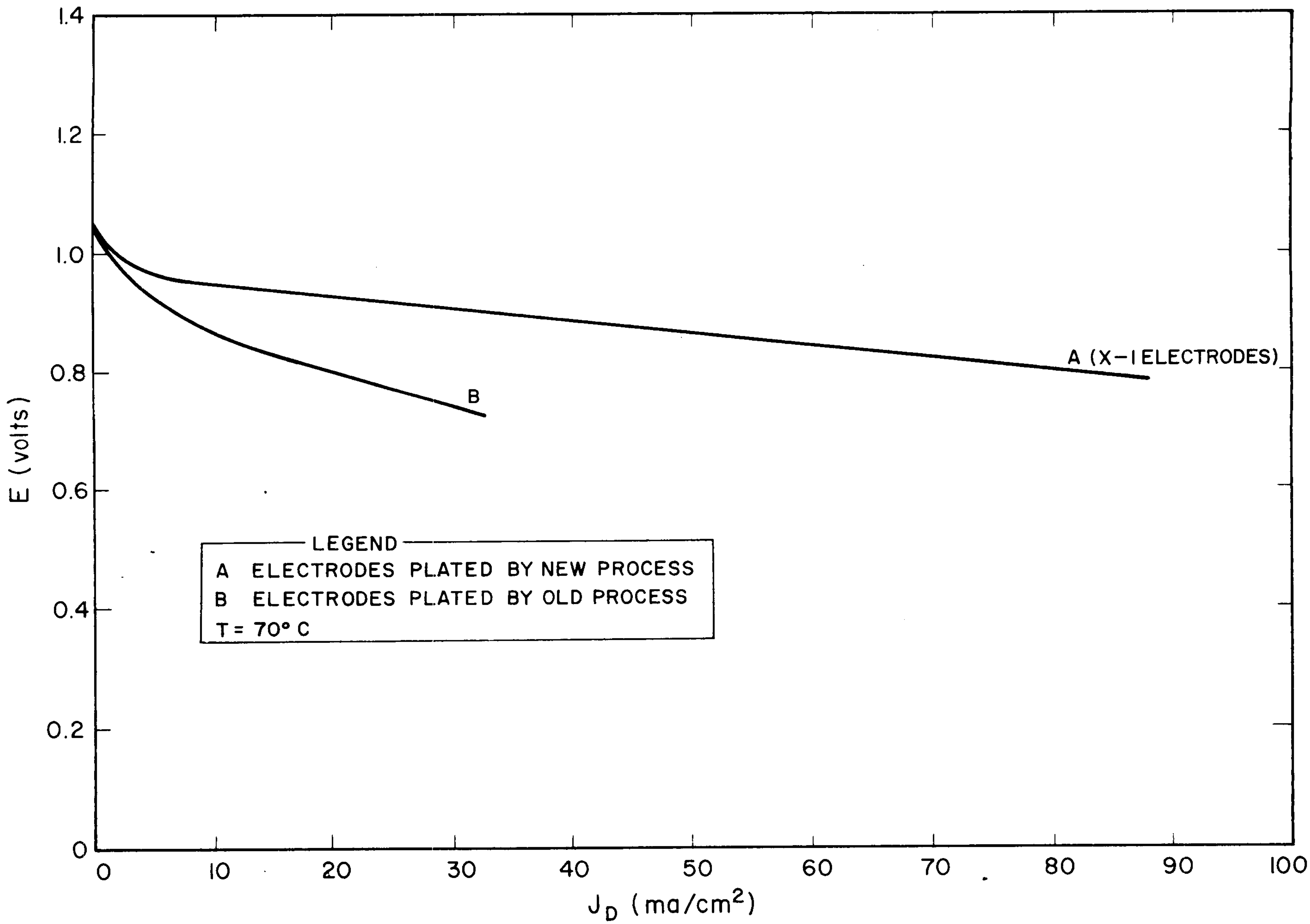

FIG. [illegible] CELL POLARIZATION CURVES WITH OLD PROCESS AND NEW PROCESS ELECTRODES

By breaking open the plated electrodes, it can be seen that these electrodes are plated all the way through by the latter process, but only on the surface by the former. Several passes of the solution through the electrode are necessary when platinum plating; the number depending on solution temperature and rate of passage. Plating with palladium is a much more rapid process, even at room temperature. Completion of the reaction is tested for in either case by treating a small portion of the filtrate with a neutral solution of KI (Ref. 2). The electrode is then washed well with hot water while in the Buchner funnel. Figure 5 shows a performance comparison between two pairs of electrodes that were made early in the program. All conditions were identical except the plating process.

The same process was used for both hydrogen and oxygen electrodes in many cases. During the program mixed catalysts were developed that gave improved performance for hydrogen electrodes and the plating procedure was modified for those electrodes. Table I gives a compilation of most of the hydrogen and oxygen electrodes used for the electrode studies. The remainder are described in the appropriate subsections.

4.2 Electrode Studies

The effects of several factors that might influence electrode performance of hydrogen-oxygen fuel cells were studied. All hydrogen electrodes and all oxygen electrodes except those for the radioactive studies were porous nickel catalyzed with platinum (or a platinum-palladium mixture in most cases) as described in Section 4.1.

The method of measuring individual electrode polarizations was described in Sections 2 and 3. It should be noted that these measurements include ohmic resistance. For all hydrogen electrodes reported in this section, the polarizations refer to the potential of the working electrode minus the potential of an exactly similar electrode in the same solution. For the oxygen electrodes, however, the irreversible nature of that electrode precludes its use as a reference and in all cases a reference electrode of Ag_2O was used. But the values reported in this section for the oxygen electrode do not represent the oxygen

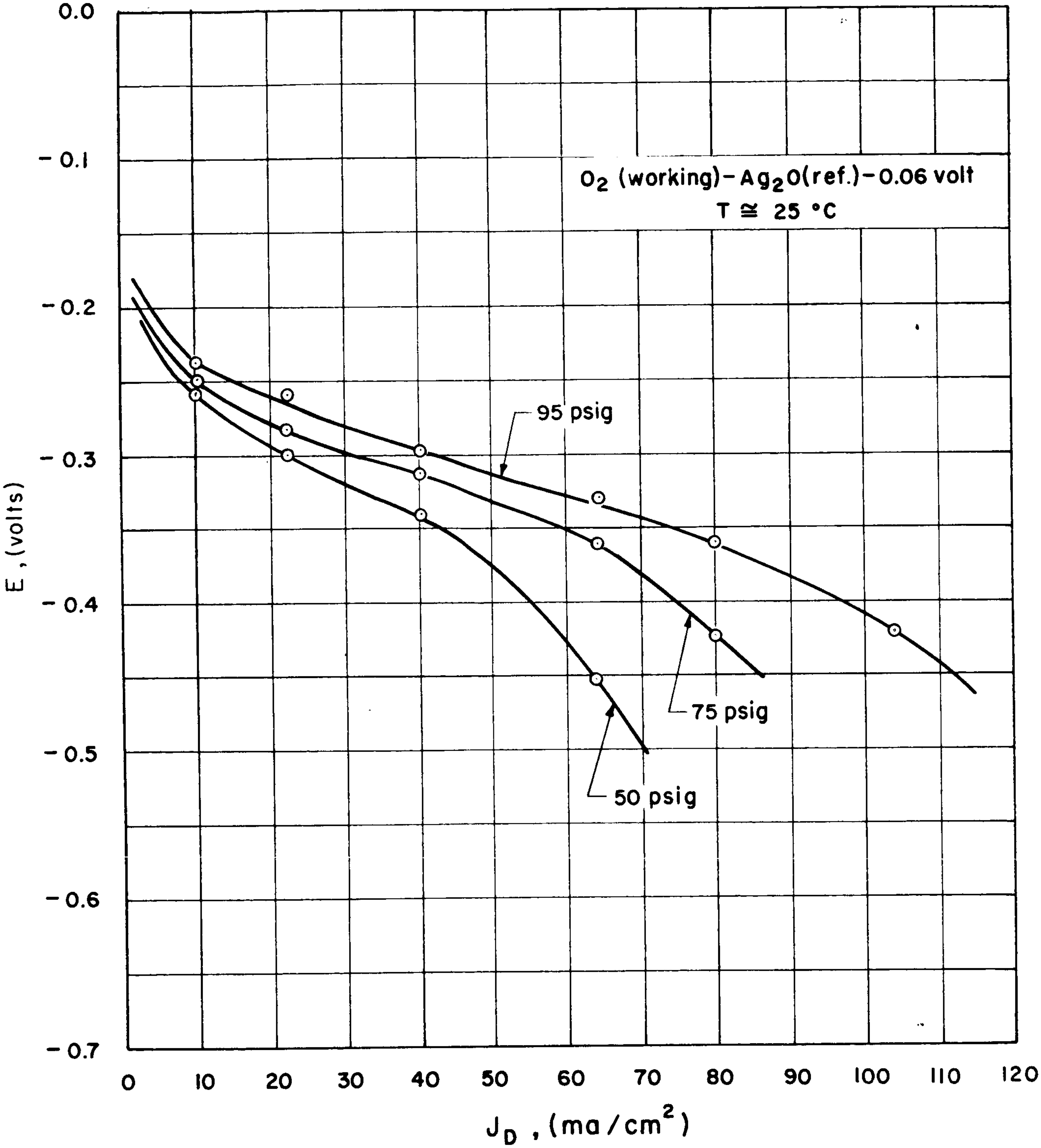

FIG. 5 PRESSURE DEPENDENCE OF AN OXYGEN ELECTRODE

TABLE I

ELECTRODE FABRICATION

FIG. NO.	TYPE ELECTRODE	CATALYST	AMOUNT OF CATALYST	TEMPERATURE	CONCENTRATION
5, 6, 9	O_2	Platinum	20 mg/cm^2	70°C ± 5°C	.84 gm $H_2PtCl_6 \cdot 6H_2O$ per 200 ml H_2O
6, 9	H_2	Platinum Palladium	5 mg/cm^2 5 mg/cm^2 10 mg Total	70°C ± 5°C	.21 gm $H_2PtCl_6 \cdot 6H_2O$ .14 gm $PdCl_2$ per 100 ml H_2O

electrode potential minus the Ag_2O potential. At unit activity of reactants, the hypothetical reversible oxygen electrode potential is 1.229 volts at 25^o and the reversible Ag_2O-Ag potential in alkaline solution is 1.172 volts (Ref. 3). The potential of O_2 vs H_2 is pH independent except at very high electrolyte concentrations where the activity of the solvent deviates significantly from unity. The potential of Ag_2O vs H_2 is approximately pH independent in alkaline solution except for effect of solvent activity as noted above and also for a minor effect due to a change of solubility of Ag_2O with pH. The hypothetical reversible potential of an actual cell will also be a weak function of the gas pressures and the temperature, but to a good approximation, under the conditions prevailing in these experiments, the reversible oxygen potential (hypothetical) will be about 0.06 volt higher than that for Ag_2O. It becomes convenient then to subtract this amount from the measured value of the O_2 (working) electrode minus the Ag_2O (reference) electrode and give plots which to a close approximation represent the extent of polarization of the oxygen electrodes. The results presented in this way are consistent with the hydrogen electrode polarization, i.e., the sum of the two electrode polarizations plus the cell potential is invariably 1.23 volts to within the accuracy of the measurements.

4.2.1 Pressure Dependence

Pressures were varied from 50 to 95 psig in these experiments. In this range, the performance of the hydrogen electrode is independent of gas pressure. The oxygen electrode, however, varies significantly within this range. The results are shown in Fig. 5. The oxygen electrode was porous nickel with 15 mg Pt/cm^2.

In addition to the effect of total pressure, it has also been found that oxygen electrodes are more sensitive to flooding than are hydrogen electrodes. If the gas pressure at either side is increased over that at the other, then the electrode at the low pressure side begins to show severe concentration polarization due to flooding. The hydrogen electrode can tolerate a differential of 1 to 2 psi while the oxygen electrode cannot. In fact, the oxygen electrode often works best if the oxygen pressure is about 1 psi higher than the hydrogen pressure. These results are presumably due to flooding and the difference in behavior of the two electrodes likely reflects the lower diffusion rate through the electrolyte film for oxygen.

4.2.2 Temperature Dependence

Polarization studies were made at 28°, 49°, and 68°C. The results are given in Figure 6. The temperature measurements were made with a chromel-alumel thermocouple whose junction was at the center of the fuel cell and about a millimeter behind the oxygen electrode. The oxygen electrode was similar to the one described in Section 4.2.1 and the hydrogen electrode was a mixed catalyst electrode as described in Section 4.2.3. The mixture was 50 percent Pt, 50 percent Pd with a total of 10 mg/cm^2 of metallic catalyst.

It will be noted that the room temperature polarization of the hydrogen electrode is somewhat greater than that for the corresponding electrode reported in Section 4.2.3. Some of the electrodes were used in a great many experiments and it has been observed that these electrodes deteriorate slowly with handling, i.e., being taken in and out of a cell. All comparative results shown in this report are for series of experiments run within as short a period as possible so that all variables could be controlled as accurately as possible. Reproduceability is usually good between identical experiments run close together in time.

Although these electrodes deteriorate gradually with handling, there is good evidence that they are stable with time, if they remain within the cell.

4.2.3 Effect of Mixed Catalysts

For hydrogen electrodes it was determined that mixed platinum-palladium catalysts are superior to either catalyst alone. A study was made in which the ratio of platinum to palladium was varied systematically. The results of the electrode polarization characteristics are shown in Figure 7 for the discharge process and in Figure 8 for the

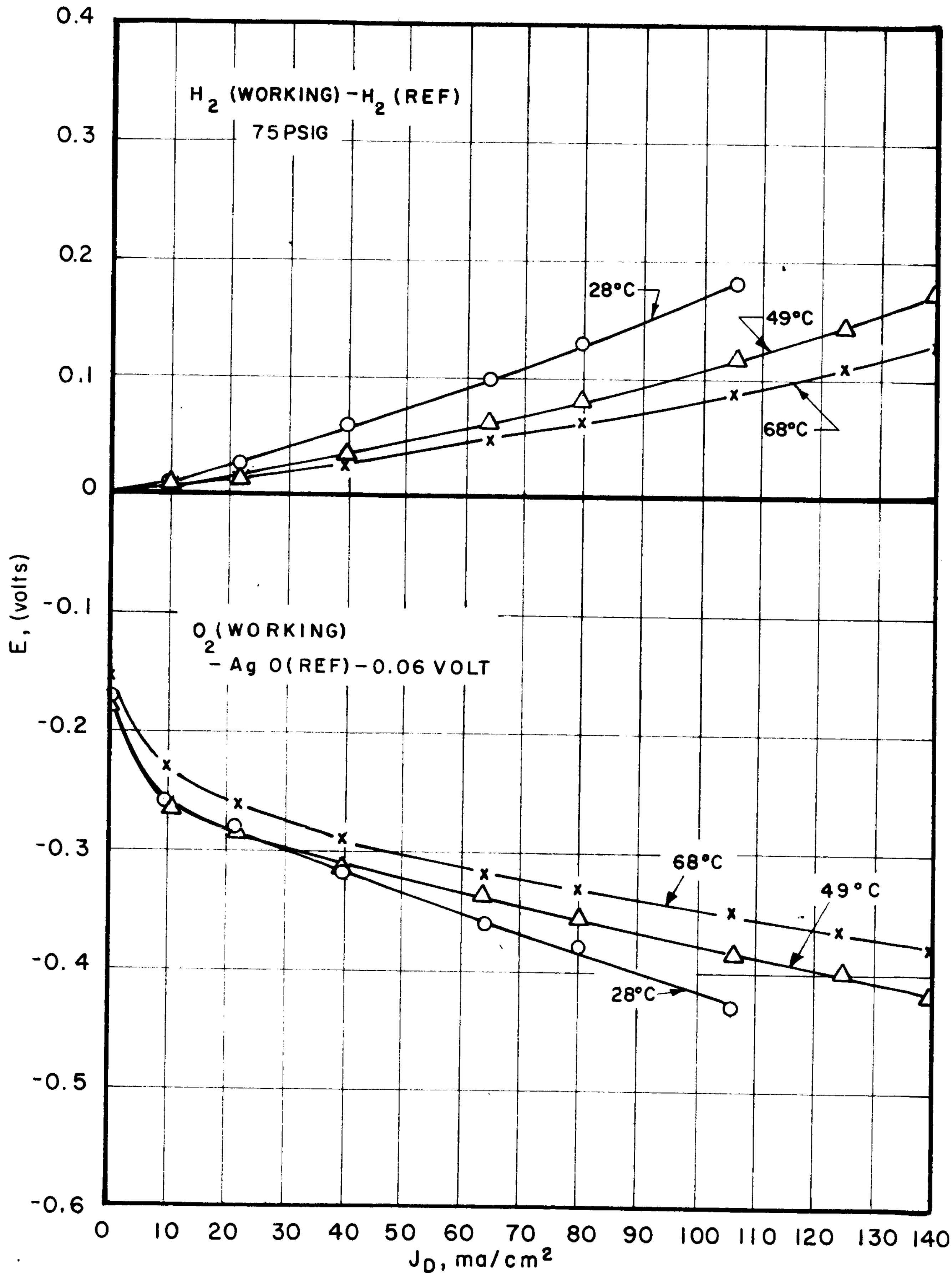

FIG. 6 TEMPERATURE DEPENDENCE OF POLARIZATION

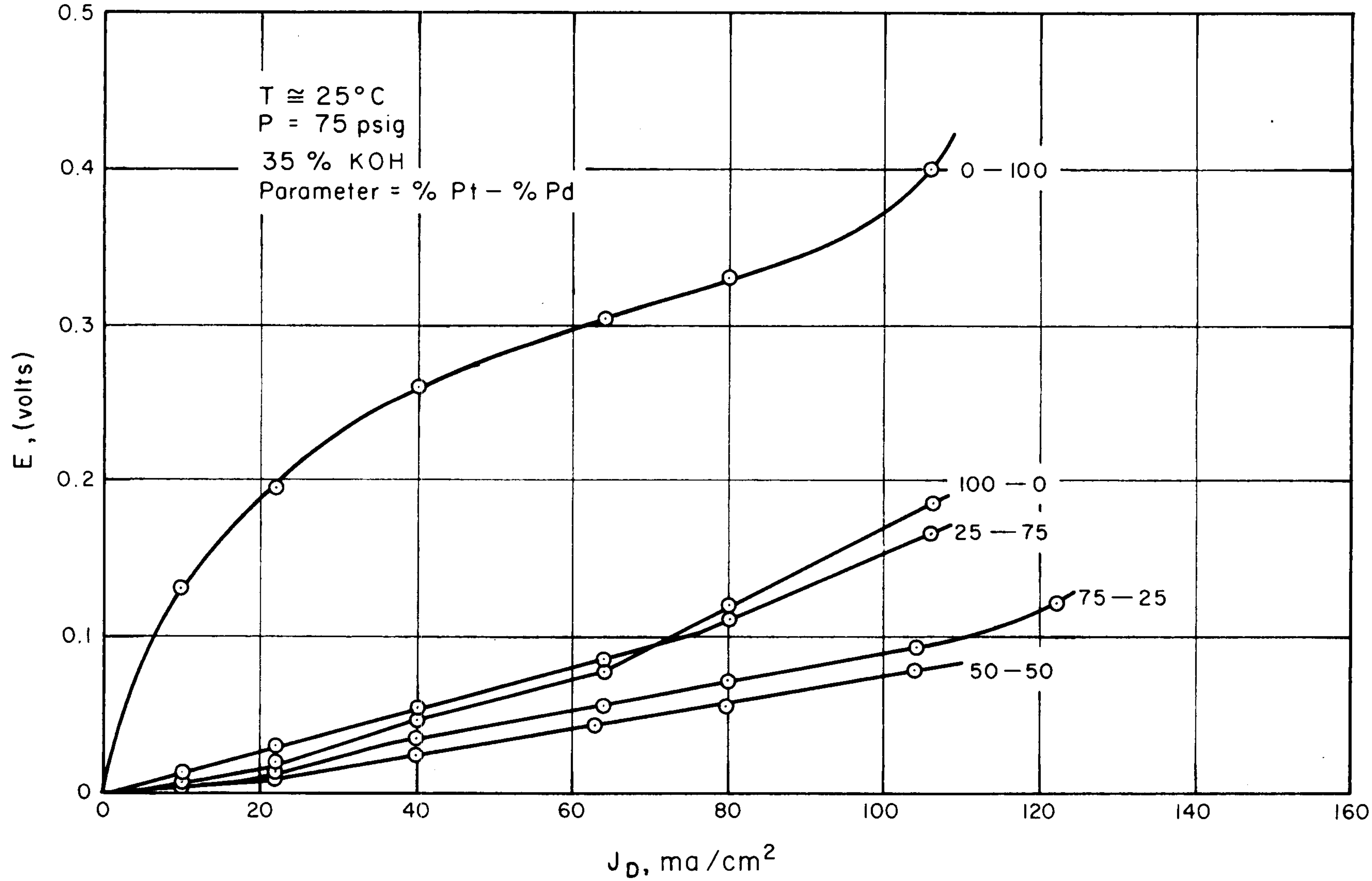

FIG. 7 HYDROGEN ELECTRODE POLARIZATION, DISCHARGE

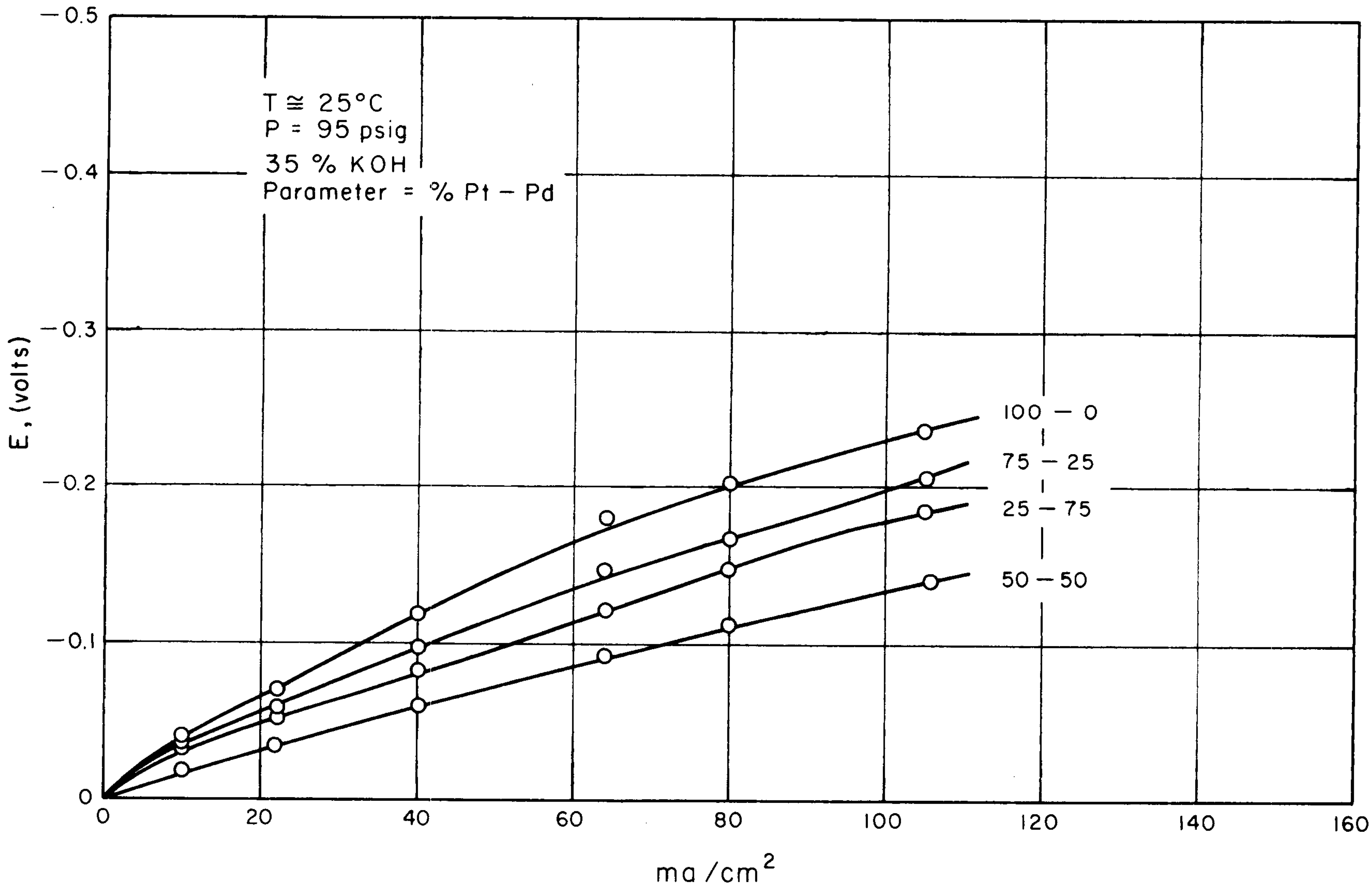

FIG. 8 HYDROGEN ELECTRODE POLARIZATION, CHARGE

charge process. The pressures were varied between 50 and 95 psig but the curves in all cases were essentially identical to the ones shown here.

It is apparent that the optimum ratio occurs at about 50 percent platinum and 50 percent palladium, but no explanation for this observation can be advanced at this time. There was, however, one fact noted in connection with electrodes plated with the mixed catalysts. They are visibly blacker than electrodes with only one catalyst and their enhanced activity may be associated with the manner in which the activating metal plates out. Thus, the coplating of palladium along with platinum might result in a finer particle size.

There was no corresponding series of experiments made with oxygen electrodes, but some observations on over-all cell potential (made in a cell without reference electrodes) would indicate that the effect is minimal.

The plating itself was accomplished by the method described in Section 4.1, but the plating solution was a mixture of $H_2P_tCl_6$ and $PdCl_2$. The amount of metallic catalyst totaled 10 mg/cm^2 in every case except for the electrode with palladium alone, which had 7.7 mg/cm^2.

4.2.4 Electrolyte Purity

The reagent grade KOH used in these experiments contained enough carbonate that a 35 percent solution made from water free from CO_2 has a $CO_3^=$ concentration of about 0.032 M. Cells with the least polarization were obtained using an electrolyte free from carbonate. In order to remove the carbonate ion from the electrolyte, $Ba(OH)_2$ was added, which precipitated carbonate as $BaCO_3$. This was allowed to settle and the solution was used from the top. In order to ascertain the effect of an excess of either Ba^{++} or $CO_3^=$, experiments were performed in which various known concentrations of Ba^{++} or $CO_3^=$ were present. The results are shown in Fig. 9. The solutions were prepared by disolving reagent grade KOH in distilled water. The solutions were then analyzed by titrating with HCl first to a phenolphthalein end point and then to a methyl orange end point. The first end

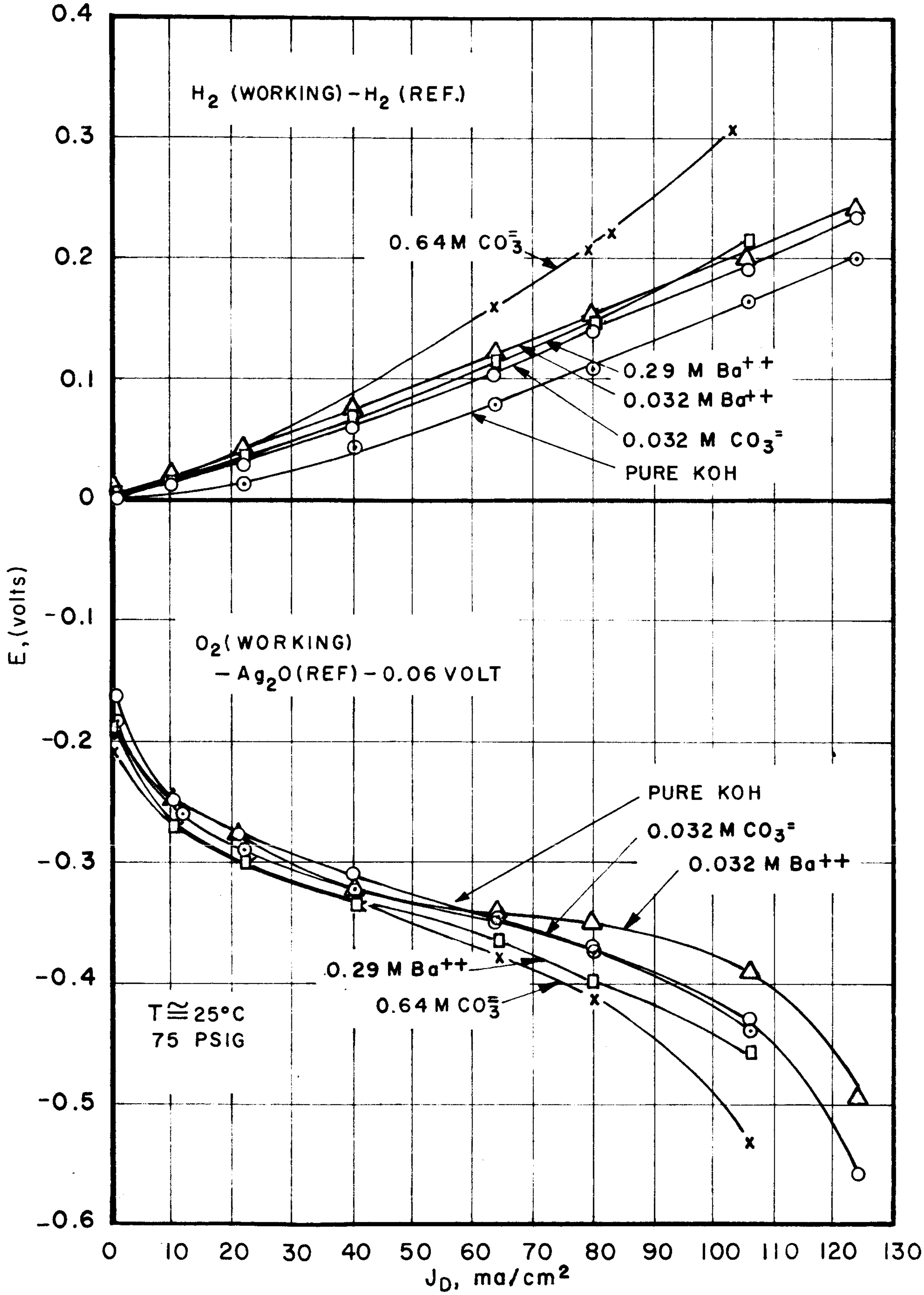

FIG. 9 EFFECT OF ELECTROLYTE PURITY ON ELECTRODE POLARIZATION

point indicates the titration of hydroxyl and bicarbonate and the latter the titration of carbonate. The appropriate amount of either K_2CO_3 or $Ba(OH)_2$ was then added to obtain the desired solution.

The experiments were run several times, and although the curves of Fig. 9 are the most nearly typical of any set of experiments, factors other than electrolyte purity influence reproduceability with the result that only a few real conclusions can be drawn. The following conclusions for the discharge process can be drawn:

1. High concentrations of carbonate ion always cause a considerable increase in polarization at the hydrogen electrode.
2. For the hydrogen electrode there is no consistent difference between 0.29 M Ba^{++}, 0.032 M Ba^{++}, and 0.032 M $CO_3^{=}$, but the "pure" electrolyte is generally a little better.
3. For the oxygen electrode 0.64 M $CO_3^{=}$ always causes the greatest increase, followed by 0.29 M Ba^{++}.
4. In the current density range of about 60 to 100 ma/cm^2, the oxygen electrode consistently operates best with a slight excess of barium ion, and the slope of the curve in this region is unexplainably small.

4.2.5 Electrolyte Concentration Dependence

Numerous attempts to reproduce some previous results on the effect of KOH electrolyte dependence on cell polarization have been made (EOS Report 33[illegible]-Q-[illegible]). The earlier results are shown in Fig. 10. Some features of that work have been verified, but the low cell polarization at high current densities with 10 percent KOH solutions have not been observed since the original work. More recent experiments were made with a cell containing reference electrodes whereas the former experiments did not incorporate this feature.

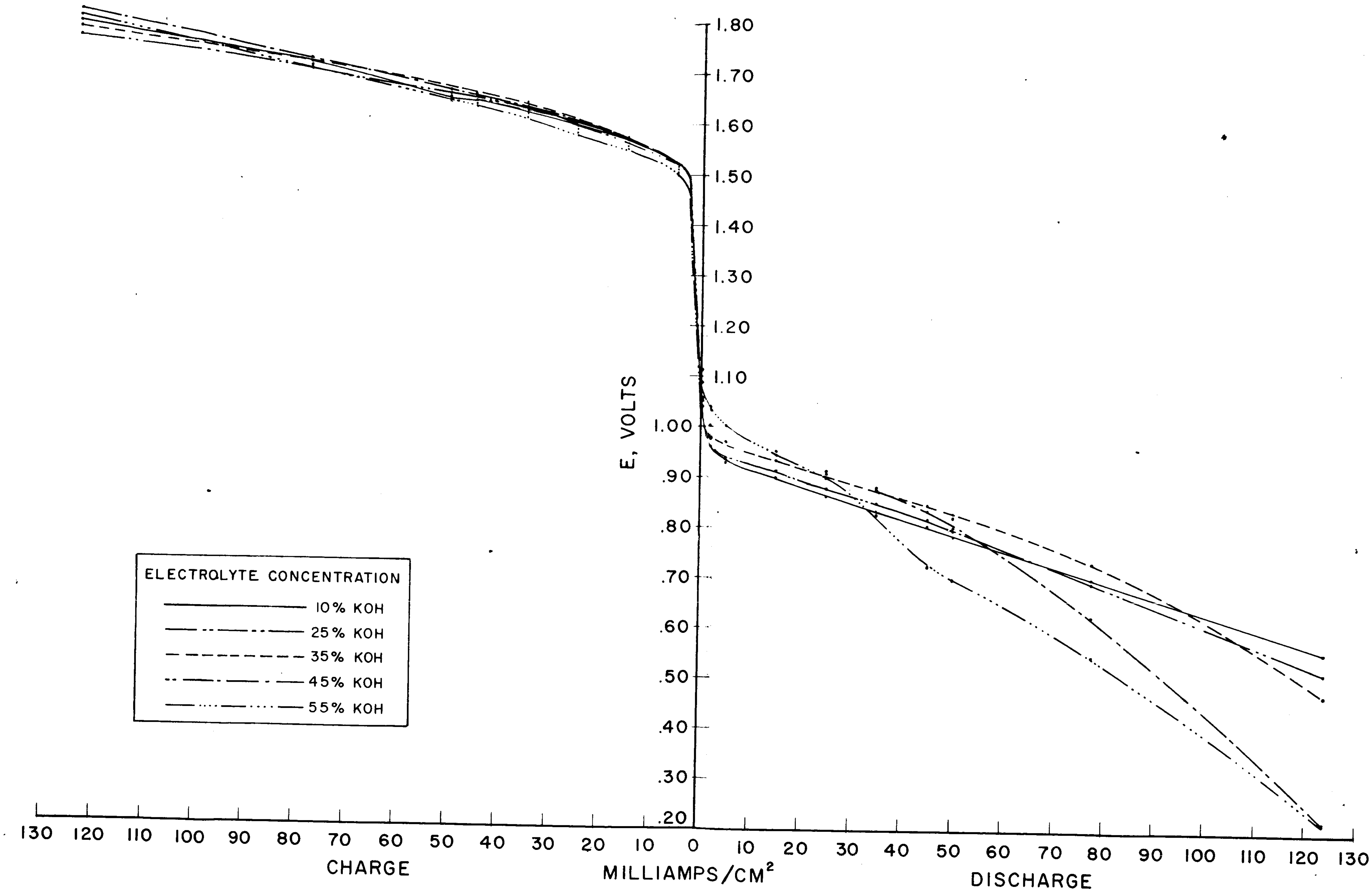

FIG. 10 CHARGE-DISCHARGE POLARIZATION H_2 O_2 CELL

Figure 11 shows the results of a series of measurements of electrode polarizations for 10 percent, 35 percent, and 55 percent KOH. The polarizations are generally somewhat higher than usual, due in part to the fact that the electrolyte had not been treated with $Ba(OH)_2$, and in part because the electrodes had been used in many previous experiments. It was found that the shape of the oxygen electrode polarization curve at 55 percent KOH, (and therefore the shape of the total cell polarization curve since the hydrogen curve is approximately linear), was very similar to the cell polarization curve reported previously. These results were usually, but not always, found. With 10 percent KOH solution on either charge or discharge, the polarizations were invariably quite high.

The importance of studies concerning the effect of electrolyte concentration on cell performance lies in the fact that a rechargeable hydrogen-oxygen fuel cell must operate over a wide concentration range. More electrolyte can be stored in a given volume if the concentration is lower, and the fraction of electrolyte which is usable water is greater; but other considerations, such as cell performance, may dictate higher initial concentrations. From the standpoint of polarization considerations, it would appear that the optimum concentration range would be from about 35 percent KOH to the saturation point.

4.2.6 Radioactive Electrodes

Four sintered silver electrodes, made from 100-200 mesh silver powder and containing a silver screen for strength, were made up for evaluating radioactive electrodes for oxygen. Three were sent to Yardney Electric Company where two of them were doped with Po^{210}, an α amitter. The third was doped with Pm^{147}, a β emitter. The fourth electrode was saved for a control. All four were tested as oxygen electrodes in a hydrogen-oxygen cell at room temperature and at 70°C. No definite correlation between radioactivity and electrode polarization was demonstrated. The results are shown in

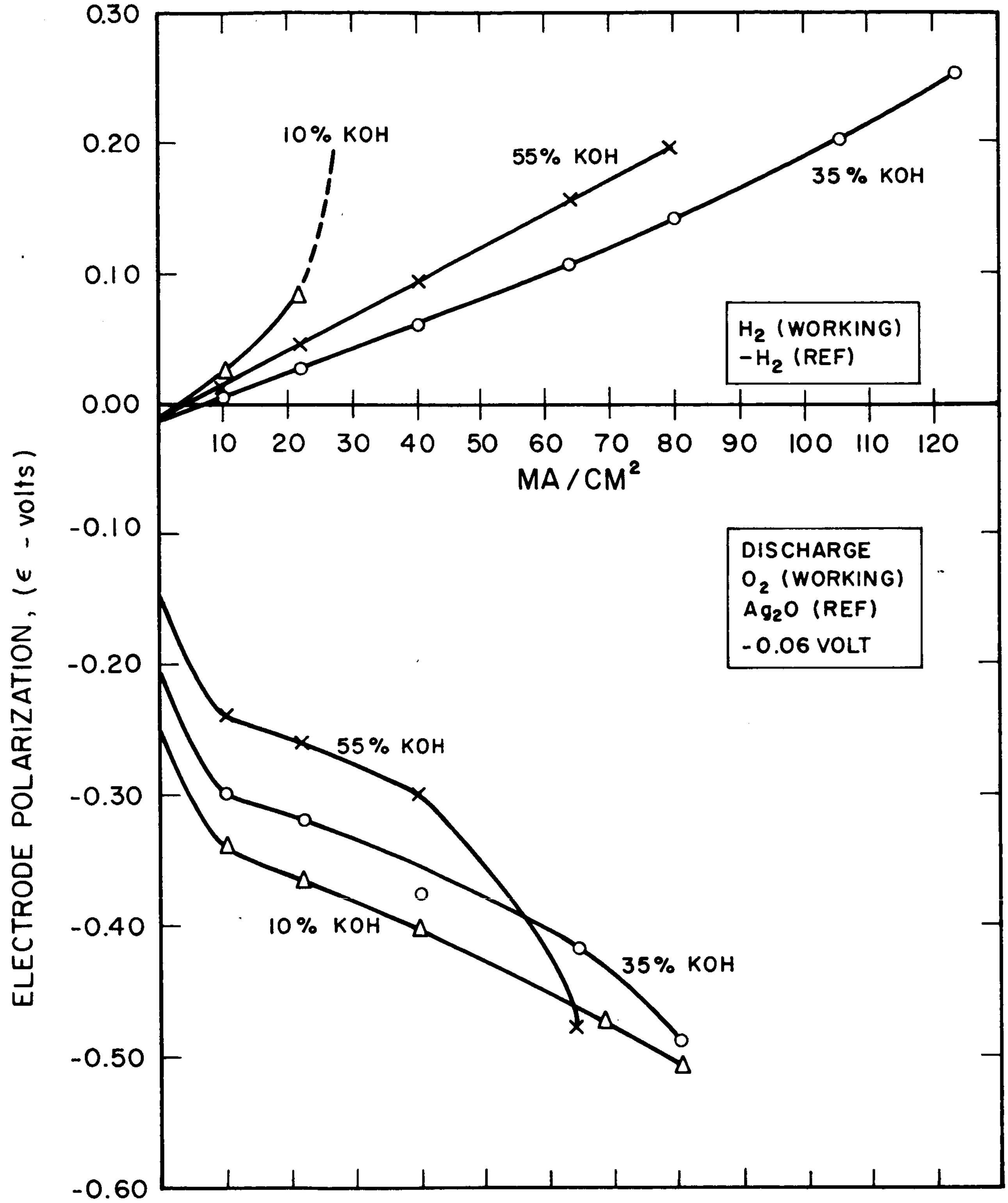

FIG. 11 EFFECT OF ELECTROLYTE CONCENTRATION ON CELL PERFORMANCE

Figs. 12 and 13, together with one of our presently used platinum blacked electrodes for comparison.

In Figs. 12 and 13, the electrode designations are as follows:

SI-1	Sintered silver, doped with Pm^{147}
SI-2	Sintered silver, doped with Po^{210}
SI-3	Sintered silver, doped with Po^{210}
SI-6	Sintered silver, undoped
X-19	Porous nickel, platinum catalyzed (15 mg/cm^2)

4.3 <u>Electrolyte Storage</u>

A cell was designed and constructed for capacity experiments. Analysis of the energy storage/weight capabilities of the hydrogen-oxygen system quickly reveals that this ratio will be limited more by the amount of stored electrolyte than by the weight of the gas storage cylinders. In all prior cells studied in this laboratory, the only electrolyte storage was between the electrodes. The new cell, shown in Figure 14, was designed to allow electrolyte storage behind the electrodes. It was postulated that the electrolyte could be moved into and out of this region by diffusional forces. The gas for each electrode was brought up through a hole in the electrolyte storage bed to a screen immediately behind the electrode. The gas port sleeves serve a triple function. They allow gas passage up to the nickel screen, where the gas is then dispersed across the entire back of the electrode, they make electrical contact to the electrode, and they determine the spacing (at least at two points) between the electrodes.

The storage behind the hydrogen electrode was made twice as much as that behind the oxygen electrode because a consideration of the individual electrode reactions shows that twice as much water is consumed or produced (for the charge or discharge process, (respectively) at the hydrogen electrode as at the oxygen electrode. These electrode reactions are:

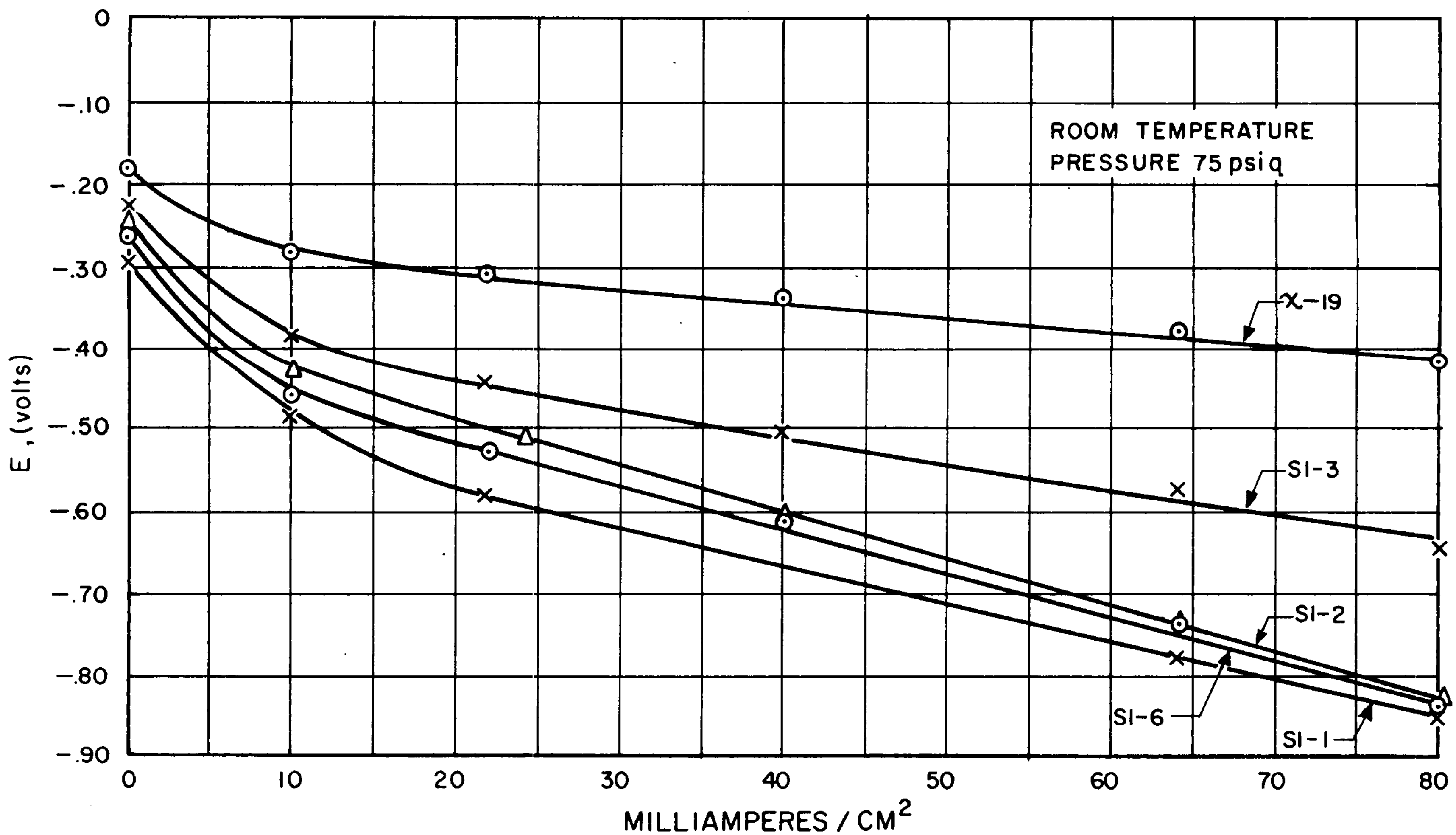

FIG. 12 POLARIZATION OF RADIOACTIVE DOPED ELECTRODES, ROOM TEMPERATURE

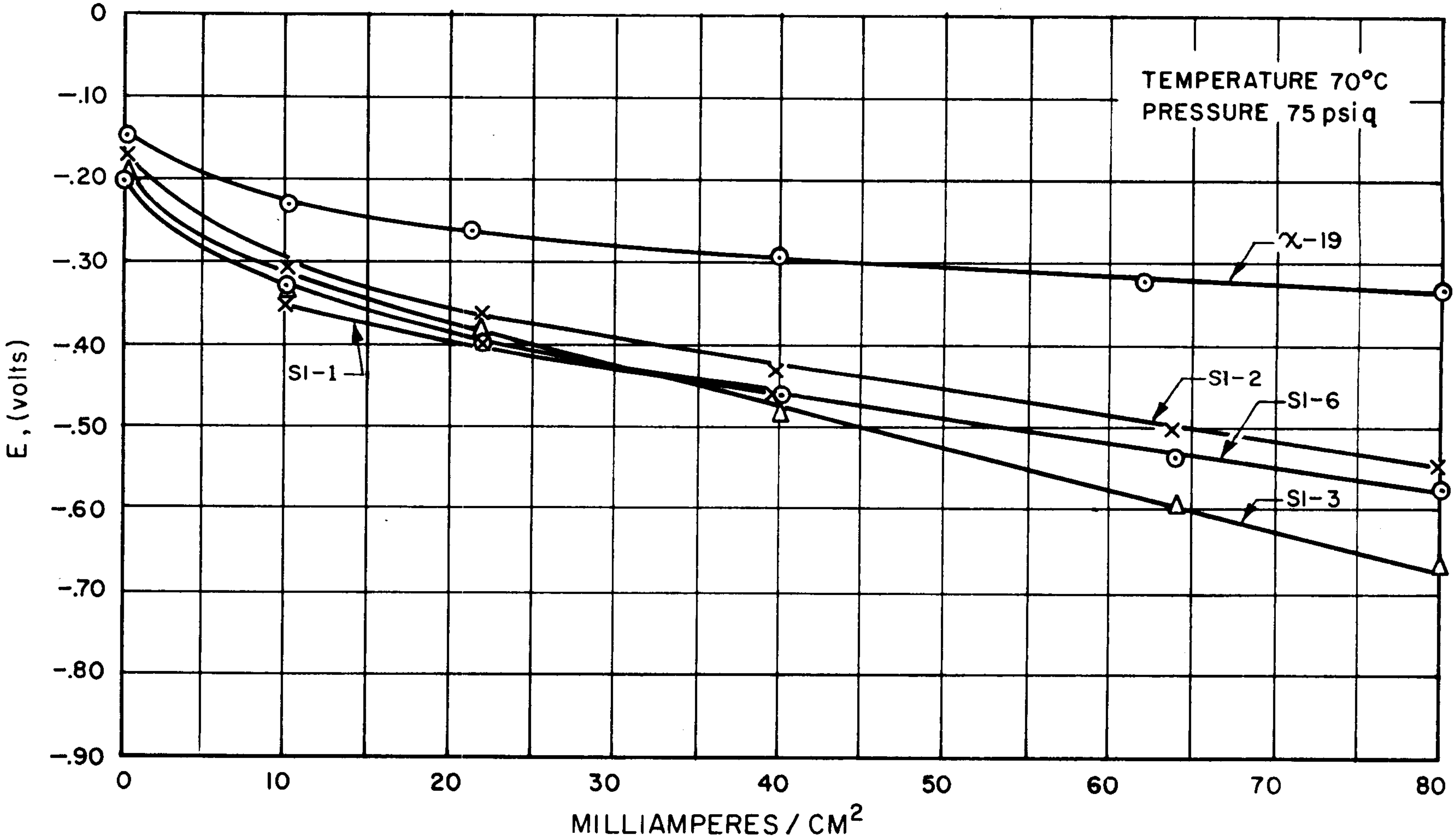

FIG. 13 POLARIZATION OF RADIOACTIVE DOPED ELECTRODES, 70°C

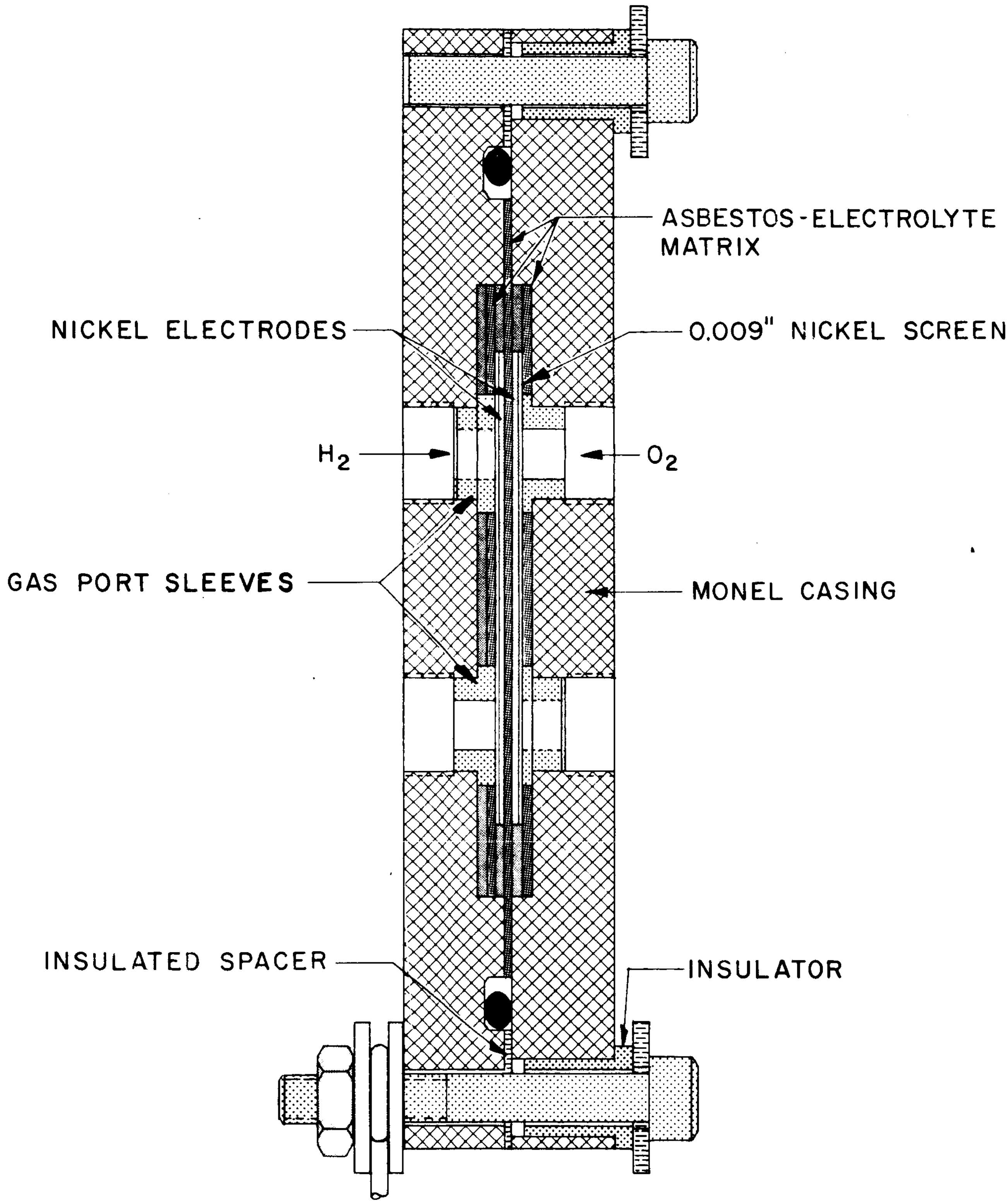

FIG. 14 HYDROGEN-OXYGEN FUEL CELL FOR ELECTROLYTE STORAGE EXPERIMENTS

$$H_2 + 2\ OH^- \underset{\text{charge}}{\overset{\text{discharge}}{\rightleftarrows}} 2\ H_2O + 2e^- \tag{1}$$

and

$$2e^- + 1/2\ O_2 + H_2O \underset{\text{charge}}{\overset{\text{discharge}}{\rightleftarrows}} 2\ OH^- \tag{2}$$

Results of these experiments are shown in Figures 15 and 16. The curves in the two figures are described in Table II. It should be noted that curves D and E are discontinuous. At the lower current densities, more than one day was required for discharge and it was considered unsafe to leave the cells on discharge without someone in attendance. This is because the nature of the constant-current power supply is such that if the cell should fail (i.e., be unable to maintain a positive potential) the power supply will charge the cell in reverse, producing hydrogen on the oxygen side and vice versa. All other discharge runs were continuous, as were all of the charges. The discharge pressure was 90 psig. When the cells were charged, they were vented to the atmosphere. This procedure prevented thermal recombination by gas diffusion.

It is interesting to note that the limit of solubility of KOH in water at 30°C (the estimated temperature within the cell) is reached when approximately 54 percent of the water has been removed, assuming KOH does not form a super-saturated solution. But in a charging operation, it can be seen that precipitation of KOH within the cell does not adversely affect electrode overvoltages.

Experiments were conducted to test the feasibility of picking up electrolyte from the back surface of the electrodes. Five holes, each about 3/16-inch in diameter, were cut in the nickel screens behind the electrodes and filled with asbestos. The results are shown in curves D and F. It will be noted that D is a real improvement over E and also that curve F (a room temperature experiment), was slightly better than G (a 70°C experiment).

The results of the experiments show unequivically that the electrolyte stored in the region behind the electrodes is available,

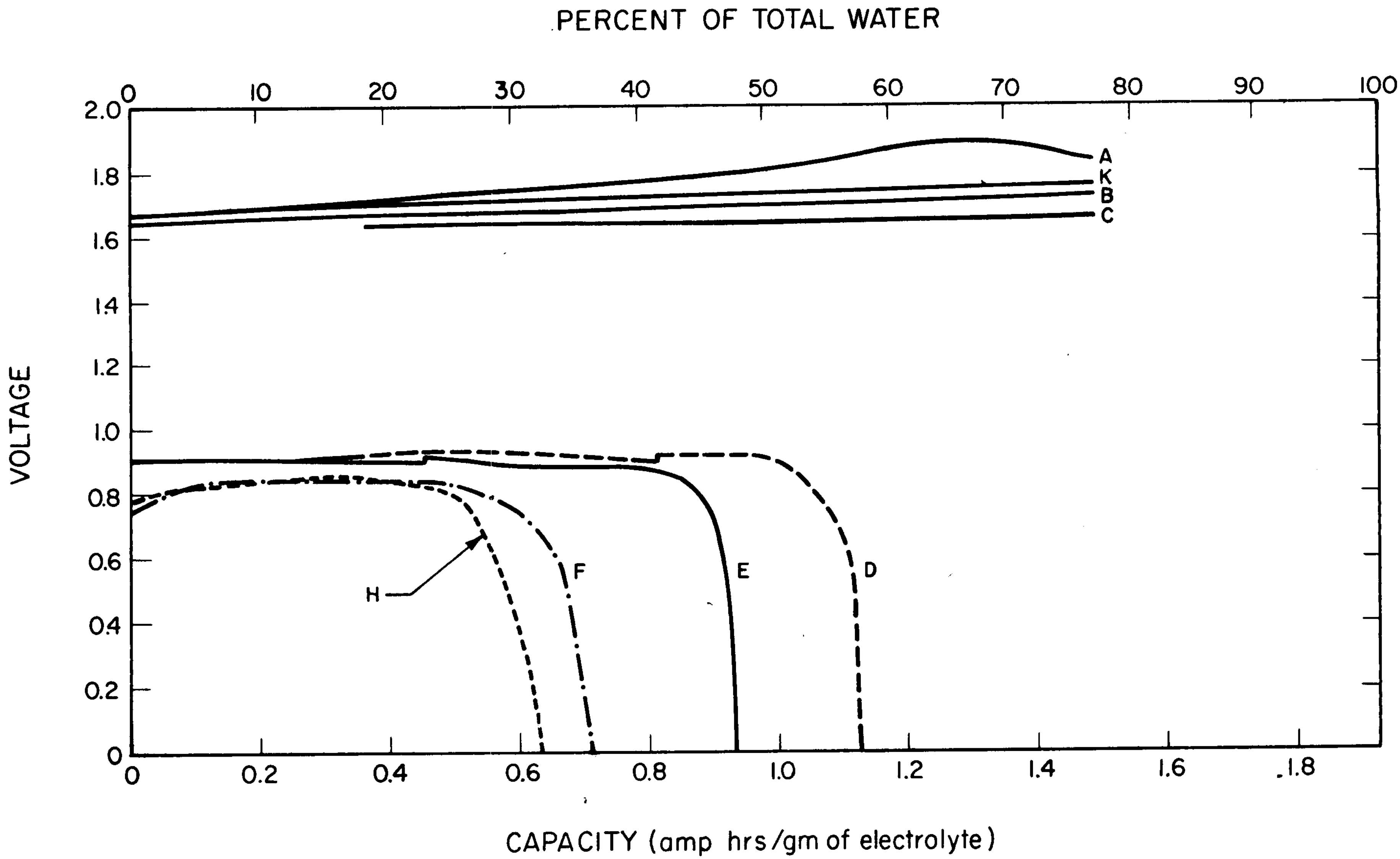

FIG. 15 CHARGE AND DISCHARGE CAPACITIES, ROOM TEMPERATURE

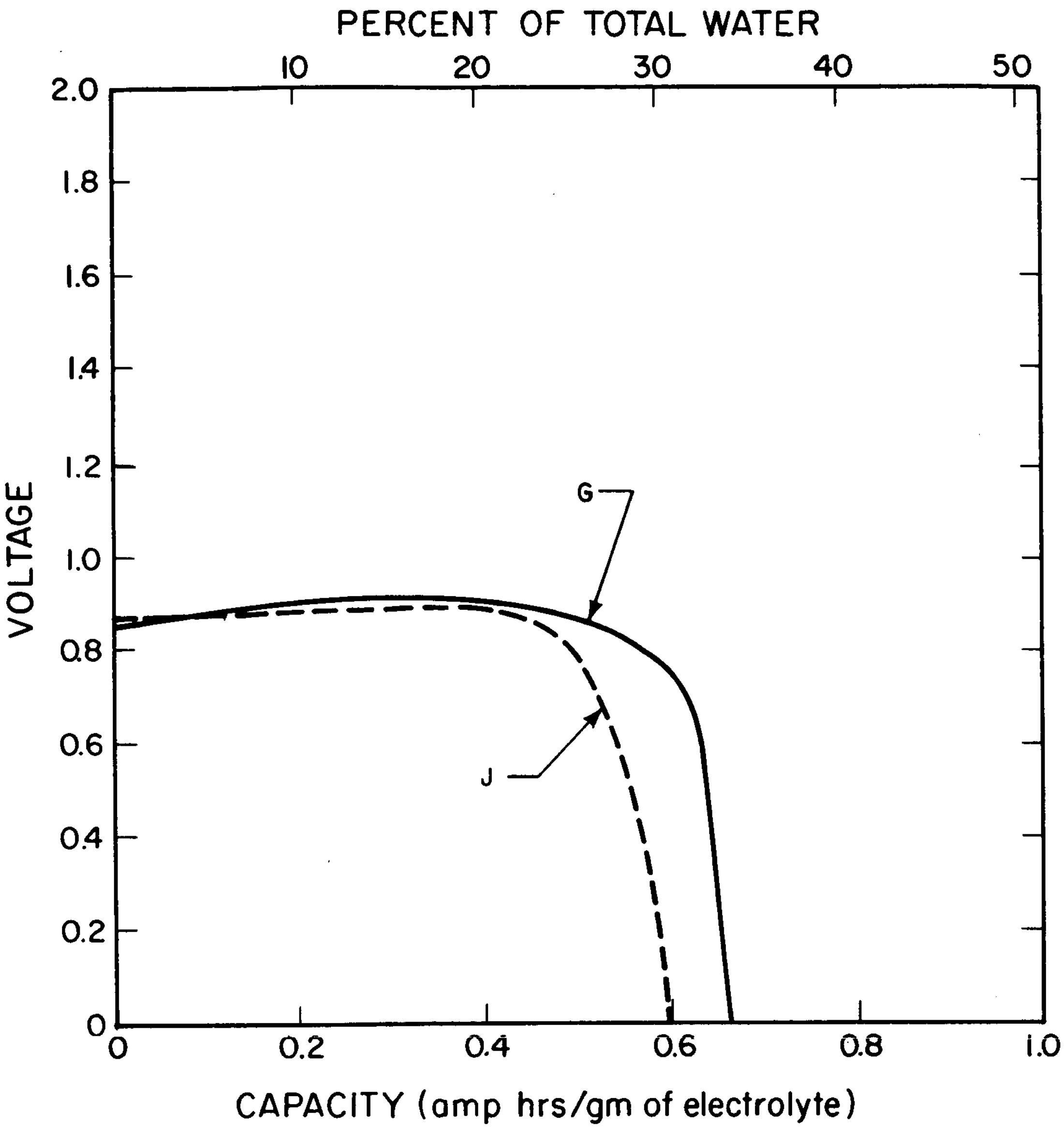

FIG. 16 DISCHARGE CAPACITY, 70°C

TABLE II

DESCRIPTION OF CURVES FOR FIGURES 15 AND 16

Curve	Exp. No.	Charge or Discharge	Temperature	Current Density	Final Electrolyte Concentration	% H_2O Consumed
A	60	Charge	Room temp.	25 ma/cm^2	54 %	77
B	63	"	" "	20 ma/cm^2	54 %	77
C	64	"	" "	25 ma/cm^2	54 %	77
D*	60	Discharge	" "	20 ma/cm^2		
E	57	"	" "	20 ma/cm^2		
F*	63	"	" "	40 ma/cm^2		
G	64	"	70°C	40 ma/cm^2		
H	64a	"	Room temp.	40 ma/cm^2		
J	66	"	70°C	40 ma/cm^2		
K	66	Charge	Room temp.	38 ma/cm^2	54 %	

* Modified screens behind the electrodes.

NOTE: The original electrolyte was 35 percent KOH in all cases for the charging operations. The final concentrations for the discharge experiments are unknown since the extent of thermal recombination is not known.

at least to some extent, for use in the cell. The total weight of 35 percent KOH solution in the cells was 6.2 gm. The total amount of electrolyte stored in the cell, exclusive of that behind the electrodes, is enough for only about 3.4 amp-hrs. By multiplying amp-hours per gram in Figures 15 and 16 by 6.2, it is seen that all curves exceed 3.4 amp-hrs.

It might seem unreasonable that at the higher temperature greater capacity was not realized. In every case the cells were previously charged to about 9.3 amp-hrs, at which point the electrolyte bed is very dry. The initial phase of discharging the cell at room temperature is always slightly unstable, but when discharging at 70°C, there is a period of more than half an hour when it is highly unstable and it is difficult to maintain equal gas pressures at the two electrodes. It is evident that under these conditions, there is considerable gas diffusion and mixing and on the highly active electrode surfaces there is considerable recombination. At 70°C, this process is more rapid and the results show that any enhanced electrolyte diffusion into the storage bed at 70°C is at least offset by greater thermal recombination. From the [illegible] discussion, it would appear that electrolyte storage [illegible] is feasible, providing an adequate solution to the gas diffusion problem is found.

4.4 Charge Retention Studies

Since charge retention is determined by the rate of gas diffusion through the electrolyte bed, an experiment was conducted to measure gas diffusion rates through the electrolyte held in an asbestos matrix. Methods used previously to measure gas diffusion rates for materials such as plastic films or membranes were not applicable to this problem since equal total pressures must be maintained at both sides of the diffusion barrier. Methods used for measuring gas diffusion through pure liquids also do not apply since the electrolyte matrix is mechanically quite different from a simple liquid film.

The conclusions drawn from the experiments reported in this section are tentative since the method employed is new and some problems associated with it are still to be resolved. In a modified procedure, which is presently being evaluated, both sides are pressurized and a slow stream of oxygen is maintained on the oxygen side. This oxygen stream passes first through a silica gel drying tube, then through a long tube in a muffle furnace packed with C O at 900°C, and then into a weighing tube packed with silica gel.

The experiment was designed so that a pressure balance to within about 0.015 psi would be maintained during the course of a determination. The principle is based on the assumption that hydrogen diffusion rates will be greater than those of either oxygen or nitrogen. A diffusion cell was first set up with hydrogen on one side and nitrogen on the other (see Fig. 17). The difference in diffusion rates for these two gases was measured by noting the volume increase on the nitrogen side as a function of time. The reading was made in a horizontal capillary tube containing mercury for the indicating liquid. The mercury was contained in a manometer with a large diameter vertical arm and a small diameter (Indicating) horizontal arm. Since these measurements gave only the difference in diffusion rates, at the conclusion of each of these experiments the gas in the nitrogen side was to be analyzed for hydrogen by the cupric oxide oxidation method. This was the reason for measuring hydrogen vs nitrogen. Further experiments of oxygen vs nitrogen would then allow calculation of the oxygen rate.

The results of the diffusion experiments indicated that under some conditions, diffusion rates are acceptable but with a relatively dry asbestos bed they are quite high. Measurements were made only on cells which were fully discharged, but different amounts of electrolyte were used.

The design of the apparatus was such that it is extremely sensitive to volume changes in either arm. For this reason, it was necessary to make careful measurements of the background leak rate before each diffusion measurement. This was done by closing two on-off valves on either side of the cell. The leak rate was almost

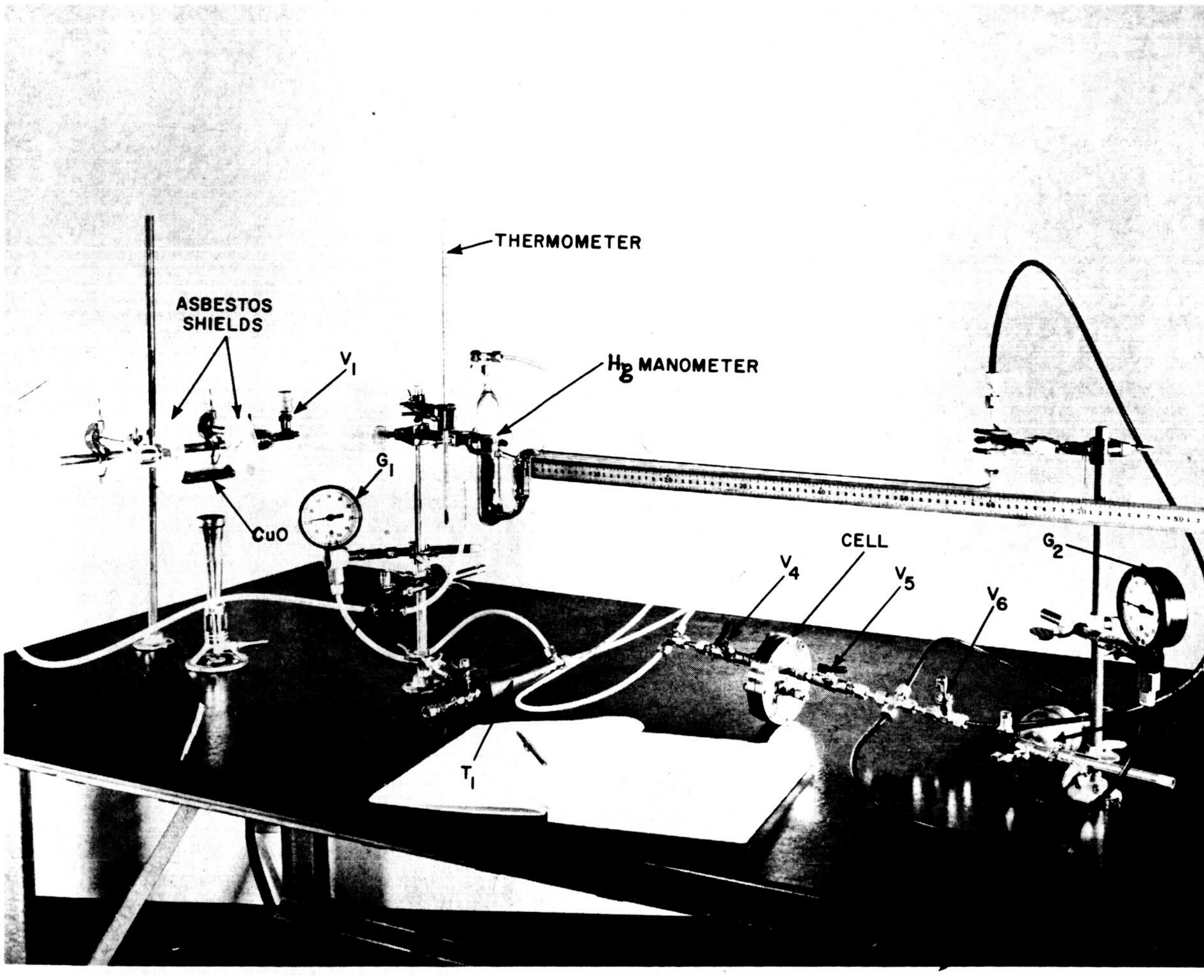

FIG. 17 GAS DIFFUSION APPARATUS

TABLE III

LIST OF GAS DIFFUSION APPARATUS SHOWN IN FIG. 17

V_1	Metering valve
V_2	Shut-off valve
V_3	Oxygen valve
V_4	On-off valve for diffusion cell
V_5	On-off valve for diffusion cell
V_6	Shut-off valve
V_7	Hydrogen valve
T_1	Oxygen tank
T_2	Hydrogen Tank
G_1	Oxygen pressure gage
G_2	Hydrogen pressure gage

always small compared to the rate of diffusion through the cell, but the main difficulty with the device was that the leak rate was not constant but varied with the amount of foreign gas (mostly hydrogen) in a given arm of the system. By making a series of measurements on the diffusion rates and extrapolating to zero time, the measured diffusion rate can be compared directly with the blank (i.e., the leak rate). This procedure is satisfactory for measuring the difference in diffusion rates, but does not allow a valid measurement of the hydrogen diffusion rate by the copper oxide method. This is because the leak rate in the nitrogen arm is variable and unknown, as it depends upon the amount of hydrogen diffused during the course of an experiment. The leak rate was such that the system lost pressure at the rate of about 0.1 psi/hr at 60 psig. There are approximately 40 joints in the system, which is made up of nylon tubing, and the logical solution would be to use an all glass system so far as possible.

The results of the measurements are summarized in Tables IV, V, and VI. In the Tables, $\Delta\ell$ is the distance the mercury column in the manometer travels in centimeters and $\Delta\ell_B$ is the distance it travels when valves V_4 and V_5 (Figure 17) are closed so that the cell is out of the system. This then is the blank, or leak rate. Experiments two through six are not reported as the system was not flushed out between runs and the measurements were not comparable.

In Table VII are shown the calculated values of the diffusion rates and diffusion coefficients. From Graham's law:

$$\frac{dn}{dt} = DA\frac{dc}{dx} \tag{3}$$

where $\frac{dn}{dt}$ is the diffusion rate, called R in Table V, D is the diffusion coefficient, c is the concentration of diffusing gas, and x is the distance through the diffusion barrier. The quantity $\frac{dc}{dx}$ is the concentration gradient and will be considered constant with time for these calculations. Because of the short time interval of the experiments

TABLE IV

DIFFUSION EXPERIMENTS, H_2 vs O_2
Matrix (.33 gm KOH per 1 gm asbestos)

Exp. No.	Pressure psig	t, mins.	Δl, cm	Δl_B, cm
1	20	0	0.0	0.0
		5	1.4	0.1
		10	4.8	0.7
		15	7.0	1.5
7	20	0	0.0	0.0
		5	3.4	1.4
		10	4.7	2.9
		15	8.7	3.7
8	40	0	0.0	0.0
		5	9.2	0.7
		10	16.2	1.6
		15	24.2	4.7
9	60	0	0.0	0.0
		5	7.8	4.0
		10	14.3	7.0
		15	18.8	8.7
10	80	0	0.0	0.0
		5	10.3	1.3
		10	17.9	2.9
		15	25.7	3.7
11	100	0	0.0	0.0
		5	3.5	1.4
		10	7.0	2.9
		15	10.2	4.0

TABLE V

DIFFUSION EXPERIMENTS, H_2 vs O_2

Matrix (.68 gm KOH per 1 gm asbestos)

Exp. No.	Press. psig	t, mins.	$\Delta \ell$, cm	$\Delta \ell_B$, cm	Exp. No.	Press. psig	t, mins.	$\Delta \ell$, cm	$\Delta \ell_B$, cm
19	20	0	0.0	0.0	22	60	0	0.0	0.0
		2	0.4	0.6			2	0.3	0.2
		4	0.9	0.7			4	0.5	0.3
		6	1.2	1.0			6	0.7	0.6
		8	2.1	1.0			8	1.0	0.7
		10	2.1	1.1			10	1.1	1.1
		15	2.7	1.5			15	1.8	1.5
20	20	0	0.0	0.0	23	100	0	0.0	0.0
		2	0.6	0.5			2	0.3	0.2
		4	0.9	0.9			4	0.8	0.6
		6	1.3	1.0			6	1.1	1.0
		8	1.3	1.1			8	1.4	1.1
		10	1.3	1.5			10	1.8	1.1
		15	2.7	2.3			15	2.9	1.5
21	60	0	0.0	010	24	100	0	0.0	0.0
		2	0.2	0.2			2	0.4	0.3
		4	0.6	0.7			4	0.4	0.8
		6	1.1	1.1			6	1.9	1.2
		8	1.2	1.5			8	3.5	1.8
		10	1.5	1.7			10	4.7	1.9
		15	2.1	2.4			15	7.4	2.9

TABLE VI

DIFFUSION EXPERIMENTS, H_2 vs N_2

Exp. No.	Press. psig	t, mins.	Δl, cm	Δl_B, cm
		Matrix (.33 gm KOH per 1 gm asbestos)		
13	20	0	0.0	0.0
		5	12.3	1.0
		10	20.3	3.3
		15	29.3	4.3
		30	40.8	
14	20	0	0.0	0.0
		5	9.0	1.0
		10	19.4	1.8
		15	28.0	2.8
		30	36.7	
		Matrix (.68 gm KOH per 1 gm asbestos)		
17	20	0	0.0	0.0
		5	5.0	1.0
		10	9.9	2.4
		15	14.0	3.3
		30	23.4	
18	20	0	0.0	0.0
		5	5.1	1.2
		10	9.9	1.7
		15	14.1	2.7
		30	18.6	

TABLE VII

DIFFUSION COEFFICIENTS AND DIFFUSION RATES FOR HYDROGEN, OXYGEN, AND NITROGEN

Exp. No.	Press. psig	Δl_{corr} cm	D_{H_2} cm^2/sec $\times 10^7$	D_{O_2} cm^2/sec $\times 10^7$	R_{H_2} moles/sec $\times 10^9$	R_{O_2} moles/sec $\times 10^9$
1	20	5.5	4.8	2.4	9.4	4.7
7	20	5.0	4.3	2.2	8.6	4.3
8	40	19.5	16.9	8.5	51.0	25.5
9	60	10.1	8.8	4.4	36.2	18.1
10	80	22.0	19.1	9.5	99.6	49.8
11	100	6.2	5.4	2.7	34.0	17.0
19	20	1.2	1.0	0.5	2.0	1.0
20	20	0.4	0.4	0.2	0.7	0.3
21	60	-0.3	-	-	-	-
22	60	0.3	0.3	0.2	1.1	0.5
23	100	1.4	1.2	0.6	7.7	3.8
24	100	4.5	3.9	220	24.6	12.3
13	20	25.0	21.6	10.8*	42.8	21.4*
14	20	25.2	21.8	10.9*	43.1	21.6*
17	20	10.7	9.3	4.7*	18.3	9.2*
18	20	11.4	9.9	5.0*	19.5	9.8*

*These values refer to nitrogen.

and consequent small build up of foreign gas in either arm, it is sufficient to consider only the Δ quantities and further to assume $\Delta c = C$, the concentration of a given gas at its high pressure side. Then ΔX is the thickness of the electrolyte bed, or 0.0795 cm.

If R has units of moles/sec, A has units of cm^2, ΔR is calculated from the data of Tables IV, V, and VI from the relation

$$\Delta R = \frac{0.0154\ C\Delta \ell_{corr}}{2t} \tag{4}$$

where $\Delta R = R_{H_2} - R_{X_2}$ (X_2 is either O_2 or N_2) and $\Delta \ell_{corr} = \Delta \ell - \Delta \ell_B$. The time of the experiment, t, is in seconds, the factor 0.0154 is the cross sectional area of the 1.4 mm ID capillary tube and the factor 2 is put in because of the nature of the experiment. If a small volume of gas, ΔV, diffuses from one side to the other, then the movement in the capillary will be $2\Delta V$ since ΔV is taken from one side and added to the other.

The values for the individual R's must rest upon some assumptions, inasmuch as hydrogen rates could not be measured directly, as noted above. One assumption which might be made is that these diffusional processes may resemble the diffusion of one gas within another, and thereby, by Graham's law, the diffusion coefficients of two gases would be inversely proportional to the square roots of their molecular weights. This has been approximately born out in measurements of diffusion coefficients of nitrogen and argon in pure water (Ref. 4). However, in measurements on hydrogen and nitrogen in water (Ref. 5) and on oxygen in water (Ref. 6) it is found that for a given temperature (near room temperature) hydrogen rates are less than twice those of oxygen and about three times that for nitrogen. For the purpose of calculating the individual R's, the assumption will be made that through the alkaline electrolyte matrix the following relations hold approximately:

$$R_{H_2} = 2R_{O_2} = 2R_{N_2} \tag{5}$$

Therefore

$$R_{H_2} = 2\Delta R \tag{6}$$

From Eq 3

$$D = \frac{R}{\frac{15.5C}{0.0795}} = \frac{R}{197.2C} \tag{7}$$

since $A = 15.5\ cm^2$, the area of the electrodes. It is assumed that the gases are accessible to the electrolyte bed only through the electrodes. This is the justification for setting A equal to the electrode area. For hydrogen, Eq 7 becomes,

$$D_{H_2} = \frac{2\Delta R}{197.2C} = \frac{\frac{2\left[0.0154\ C\Delta\ell_{corr}\right]}{2t}}{197.2C} \tag{8}$$

$$= 7.80 \times 10^{-5}\ \frac{\Delta\ell_{corr}}{t} \tag{9}$$

and for nitrogen or oxygen the relation is

$$D_{X_2} = 3.90 \times 10^{-5}\ \frac{\Delta\ell_{corr}}{t} \tag{10}$$

It should be noted that the diffusion coefficients are independent of pressure. The rates, however, are pressure dependent and are given by

$$R_{H_2} = 2\Delta R = 0.0154\ \frac{C\Delta\ell_{corr}}{t} \tag{11}$$

and $$R_{X_2} = \Delta R = 0.0077\ \frac{C\Delta\ell_{corr}}{t} \tag{12}$$

Table VII shows values of the diffusion coefficients and diffusion rates for the experiments which were preformed. The diffusion coefficients for these gases in pure water at room temperature lie in the range of about 2 to 5 x 10^{-5} cm^2/sec. The diffusion rates, which are pressure dependent, for the values reported in Table VII correspond to currents of the order of 0.1 to 1.0 ma/cm^2. Consider, for example, Exp. No. 9 (Table VII)

$$R_{H_2} \cong 36 \times 10^{-9} \text{ moles/sec}$$

This amount of hydrogen would react thermally with oxygen to form 36×10^{-9} moles/sec of water.

$$R_{O_2} \cong 18 \times 10^{-9} \text{ moles/sec}$$

This oxygen would react thermally with hydrogen to form 36×10^{-9} moles/sec of water. Therefore, $(36 + 36) \times 10^{-9}$ or 72×10^{-9} moles/sec of water would be formed for 15.5 cm^2 of electrode area, so that about 4.6×10^{-9} moles/sec is the self-discharge rate. One mole of water formed per second is equivalent to 2 x 96, 500 or 193,000 amps. Therefore, in terms of an equivalent self-discharge current density, 4.6×10^{-9} moles/sec/cm^2 = $4.6 \times 10^{-9} \times 1.93 \times 10^5 \times 10^3 = 0.9$ ma/cm^2. The efficiency loss caused by a self-discharge rate of this magnitude would be acceptable under most circumstances, but the diffusion rates would very likely be higher (perhaps much higher) at high states of charge and high pressure. Several electrolytically conductive membranes are being looked at presently in this laboratory for the purpose of acting as diffusion barriers when placed between layers of the asbestos. Some of the results to date look promising.

4.5 Cycle Efficiency Measurements

Some experiments were set up for the purpose of determining the current efficiency of a cell while undergoing a charge-discharge cycle. In one experiment, a cell was charged with 1.8 gm of 35 percent KOH solution, as this had previously been determined as the maximum amount for that size cell in order to achieve minimum electrode polarization. A pressure of 50 psig was applied and the cell was then charged to 1.59 amp-hrs and immediately discharged. Only 0.74 amp-hrs discharge was obtained to the starting pressure, but there was apparently a leak in the pressure equalizer. Another experiment was performed without the equalizer and more electrolyte in the bed. The cell was charged for 0.39 amp-hr and discharged to 0.37 amp-hr, or 95 percent of the original charge. Thus, it is seen that current efficiency in cyclic operation can be high, but with the present design considerably more than the optimum amount of electrolyte is needed in the bed.

5. HYDROGEN-SILVER OXIDE CELLS

The hydrogen-silver oxide cell studies were concerned with increasing cell performance and increasing the capacity of the silver electrode on the first charging plateau (i.e., during the oxidation of silver to Ag_2O). The importance of this is that higher efficiency and longer lived cells would result if the charging and discharging could be carried out only in the first plateau without paying a large penalty in a lowered energy/weight ratio. Since there is only one gas stored (hydrogen) it would be desirable to store it in other than a gaseous form. The resulting cell would then have no gas storage. Therefore, the studies also included hydrogen storage in palladium and in Raney nickel.

In order to improve the polarization characteristics and capacity on the first charging plateau of a silver oxide electrode, experiments were conducted on the effect of doping the silver oxide. There is evidence that the capacity on the first plateau is limited by the high resistivity of Ag_2O. Thus, a prevalent theory to account for the fact that much less than the theoretical charge is accepted on the first plateau is as follows: oxidation of Ag to Ag_2O occurs only on the surface, and when the surface of the electrode becomes completely covered by the high resistance film of Ag_2O, then Ag_2O is oxidized to AgO and the potential of the electrode increases to that of the second plateau. Essentially all of the electrode can now be oxidized since the AgO formed can thermally oxidize Ag to Ag_2O and itself be reduced to Ag_2O. The resistivity of AgO is reported to be from six to nine orders of magnitude less than that of Ag_2O, or approximately 0.01 to 10 ohm-cm (Ref. 7). That the high resistivity of Ag_2O is responsible for the limited capacity on the first plateau, and not some other factor such as availability of electrolyte, is demonstrated by some observations by T. P. Dirkse (Ref. 8). It has been our observation, as well as that of Dirkse, (Ref. 7), that the electrochemical action occurs outward from the grid or, in the case of most of our cells, from the contact between the electrode and the body of the cell at the back of the electrode. On the oxidation of Ag_2O to AgO, Dirkse has this to say, "Thus, the resistance of the Ag_2O seemed to make it easier for AgO to form at the grid where the amount of electrolyte was small rather than at the electrode surface where there was plenty of electrolyte."

5.1 Electrode Fabrication

Several methods of making silver oxide electrodes were tried. One method consisted of sintering silver powder onto an expanded silver "screen" made from silver of 0.010-inch thickness. In some cases carbon was incorporated into the electrode for conductivity purposes. Two different sizes of silver powder were used, and in some cases doped oxides were made by alloying cadmium or nickel with the silver and aluminum, then powdered and sintered. The aluminum was then leached out with a KOH solution. The method of producing the individual electrodes will be given, together with the results of their tests, in Section 5.2.

Polarization and charging capacity were very poor for all of the electrodes described above except for the Raney silver electrode. The vast majority of the work on silver oxide electrodes was done with electrodes made by pasting freshly precipitated silver oxide directly into the cell. Doping of these electrodes was accomplished by coprecipitating the oxide of the doping metal. The silver grid was not used with these electrodes as the grid material differed so markedly in physical form from this finely divided oxide. Its presence would have been a great leveling factor on electrode behavior.

5.2 Silver Oxide Electrode Studies

The electrode studies consisted of polarization and charge capacity measurements on the first plateau. Resistivity measurements of pure Ag_2O and several doped oxides will also be considered here.

5.2.1 Resistivity of Doped Silver Oxide

A program was conducted in which ten samples of Ag_2O were each doped with 0.5 atom percent of a dipositive element. Their resistivities were determined and compared with that of undoped Ag_2O. Then two of the best of these were studied as silver oxide electrodes and again compared with the undoped Ag_2O.

Silver oxide was doped by a coprecipitation method. To a neutral solution of $AgNO_3$ and the nitrate of the impurity metal, a 35 percent KOH solution was added while the whole solution was being stirred with a magnetic stirrer. The solid phase solubilities of the oxides in question are in general not known, but the amount of impurity oxide formed would give 0.5 percent on an atomic basis on the assumption that its solubility in Ag_2O is that great.

Table VIII shows resistivity values at room temperature for all samples, including the undoped Ag_2O. These values represent measurements made on a single sample of each oxide. Values at 100°C are also given for the doped oxides except the cobalt doped oxide, where the resistivity was too low for the measuring apparatus and the cadmium and mercury doped oxides, where the samples were broken. The room temperature values for the latter two are, therefore, uncertain also. The samples for Table VIII were prepared by placing the slightly wet oxides in a rubber cylinder about 1 cm in diameter and exerting a hydrostatic pressure of approximately 250 psi. They were then dried overnight at 100°C and placed in a dessicator until they were ready for use. Each sample was approximately 2 mm thick but there was some variation from one to another. Silver paint was applied to the opposite faces and the resistance was measured directly by means of a Hewlett-Packard model 412AR DC vacuum tube volt meter. Resistance as high as 5×10^9 ohms could be read directly. The resistivity of Ag_2O has been reported elsewhere to be of the order of $10^{[illegible]}$ ohm-cm (Ref. 8)

TABLE VIII

RESISTIVITIES OF DOPED AND UNDOPED Ag_2O

Material	R, 25°C	ρ, 25°C	R, 100°C	ρ, 100°C
Ag_2O	1.30	5.20		
Ag_2O +0.005 ZnO	3.30	15.0	0.03	0.14
Ag_2O +0.005 CdO*	(4.90)	(20.0)		
Ag_2O +0.005 HgO*	(0.56)	(2.25)		
Ag_2O +0.005 CuO	1.46	6.30	0.02	0.09
Ag_2O +0.005 PbO	1.05	5.50	0.01	0.05
Ag_2O +0.005 PdO	0.70	4.40	< 0.01	< 0.06
Ag_2O +0.005 MnO	0.10	0.52	< 0.01	< 0.06
Ag_2O +0.005 FeO	0.81	4.50	0.02	0.11
Ag_2O +0.005 CoO	0.02	0.08		
Ag_2O +0.005 NiO	0.79	3.95	< 0.01	< 0.05

* Samples were cracked

R = resistance, 10^8 ohms

ρ = resistivity, 10^8 ohm-cm

5.2.2 Polarization and Capacity of Silver Oxide Electrodes

Some initial experiments were performed for the dual purpose of checking out the functioning of the reference electrodes and measuring the characteristics of an undoped silver oxide electrode. Constant current charging curves are given in Figs. 18, 19, 20 and 21.

The functions shown in Fig. 19 have the following meaning:

1. Ag_2O (working) - H_2 (working)
2. Ag_2O (working) - H_2 (reference)
3. Ag_2O (reference) - H_2 (reference)
4. H_2 (working) - H_2 (reference)
5. Ag_2O (working) - Ag_2O (reference)

On the second plateau, of course, the Ag_2O working electrode becomes AgO.

The theoretical potential for the reaction

$$Ag_2O + H_2 \longrightarrow 2Ag + H_2O$$

is 1.172 volts (Ref. 3). The fact that channel No. 3 reads very close to this value for most experiments was taken as evidence that both reference electrodes are highly reversible and unpolarized. It can be seen that large currents flowing between the working electrodes have no effect on the potential of the two reference electrodes. Separate experiments, conducted on several occasions, established that they are unaffected to at least 220 ma/cm^2 flowing in the cell. On some occasions, however, polarization of one or the other reference electrode was noticed. Departure of channel No. 3 from the reversible value indicates that at least one reference electrode has become polarized. Every failure of the Ag_2O reference electrode has occurred because of its reduction. This can be detected by channel No. 5, which then goes to zero. Also, channel No. 3 falls off by an amount equal to the polarization of the Ag_2O. It would sometimes happen

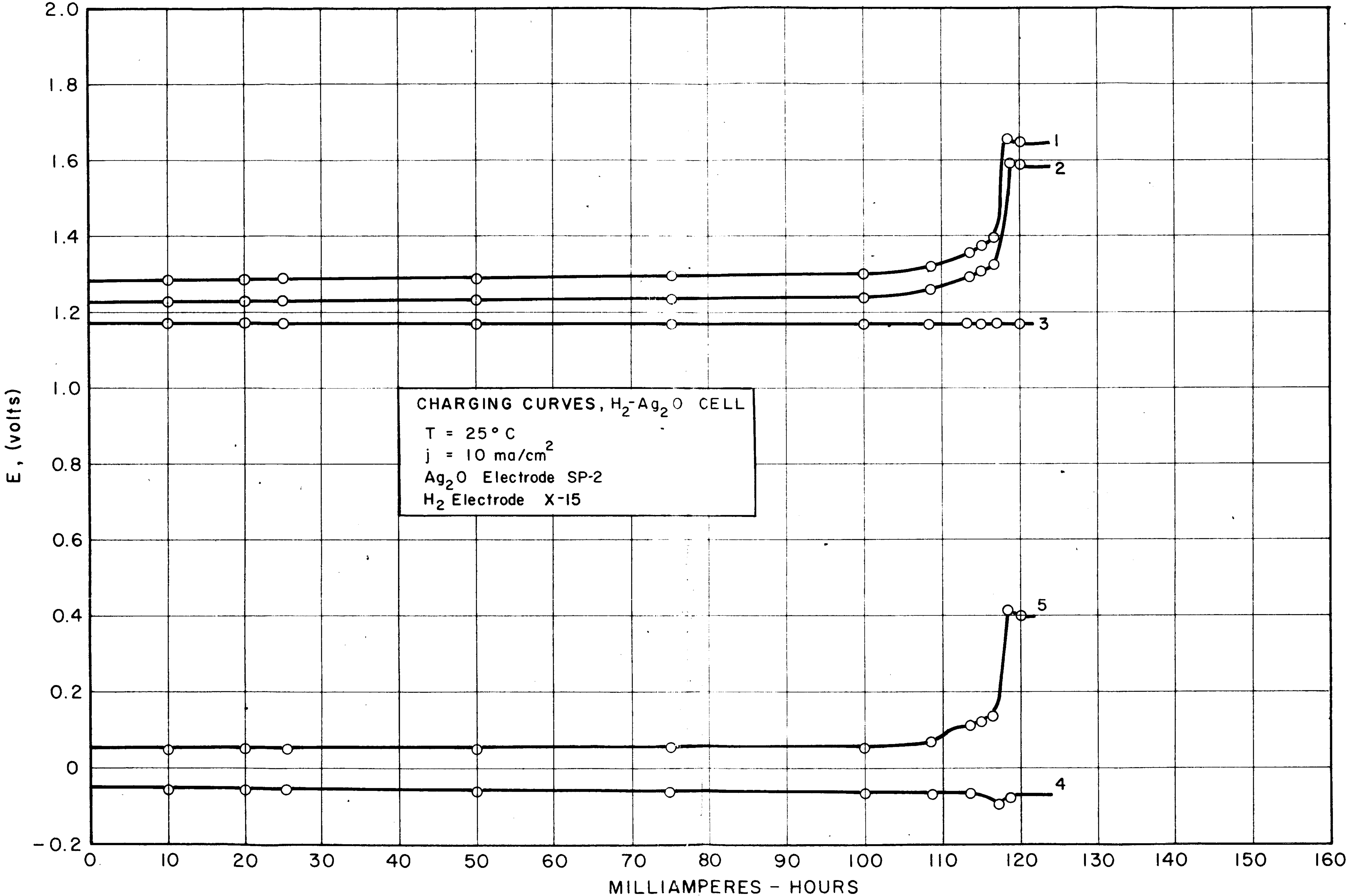

FIG. 18 CHARGING CURVES, HYDROGEN-SILVER OXIDE CELL

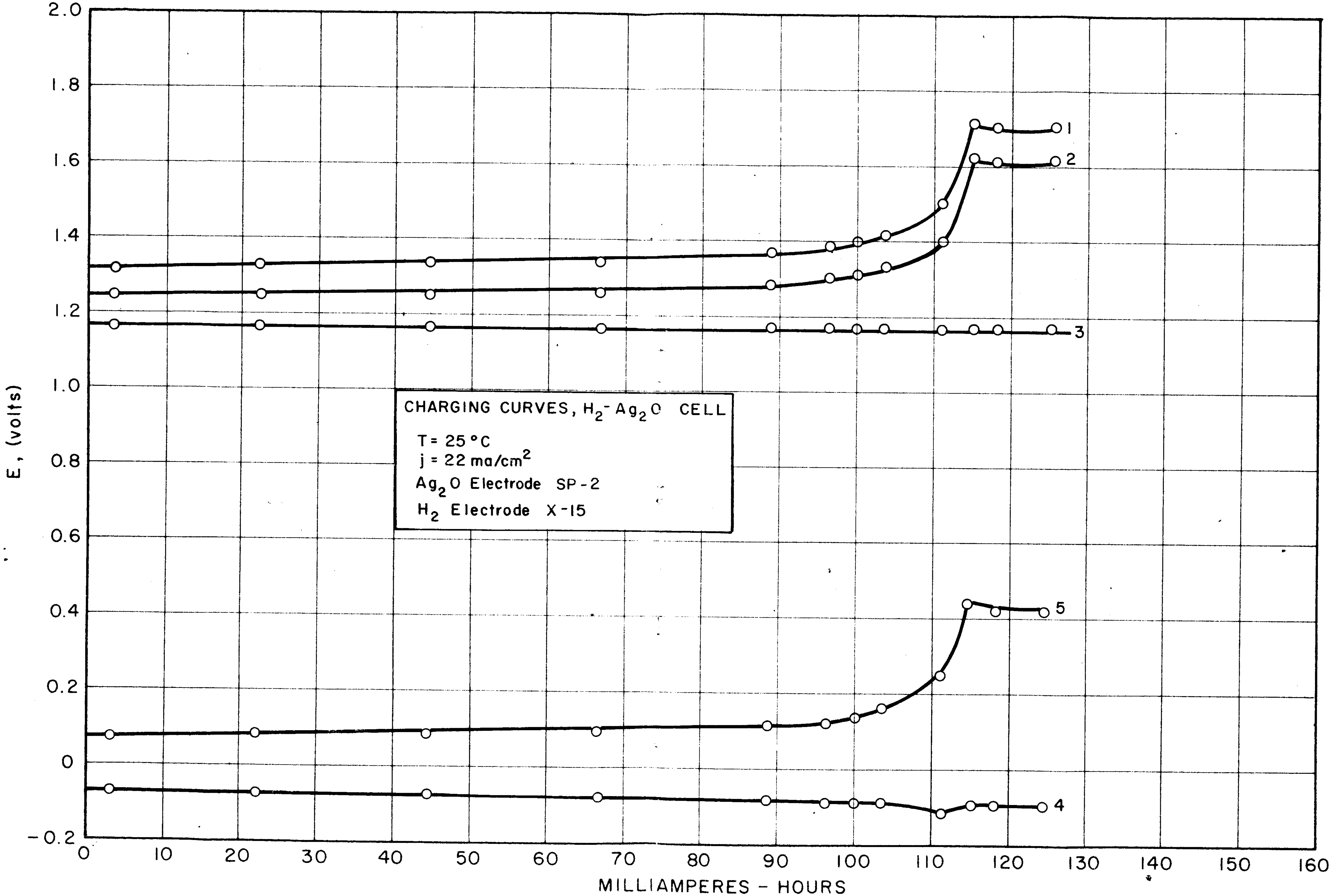

FIG. 19 CHARGING CURVES, HYDROGEN-SILVER OXIDE CELL

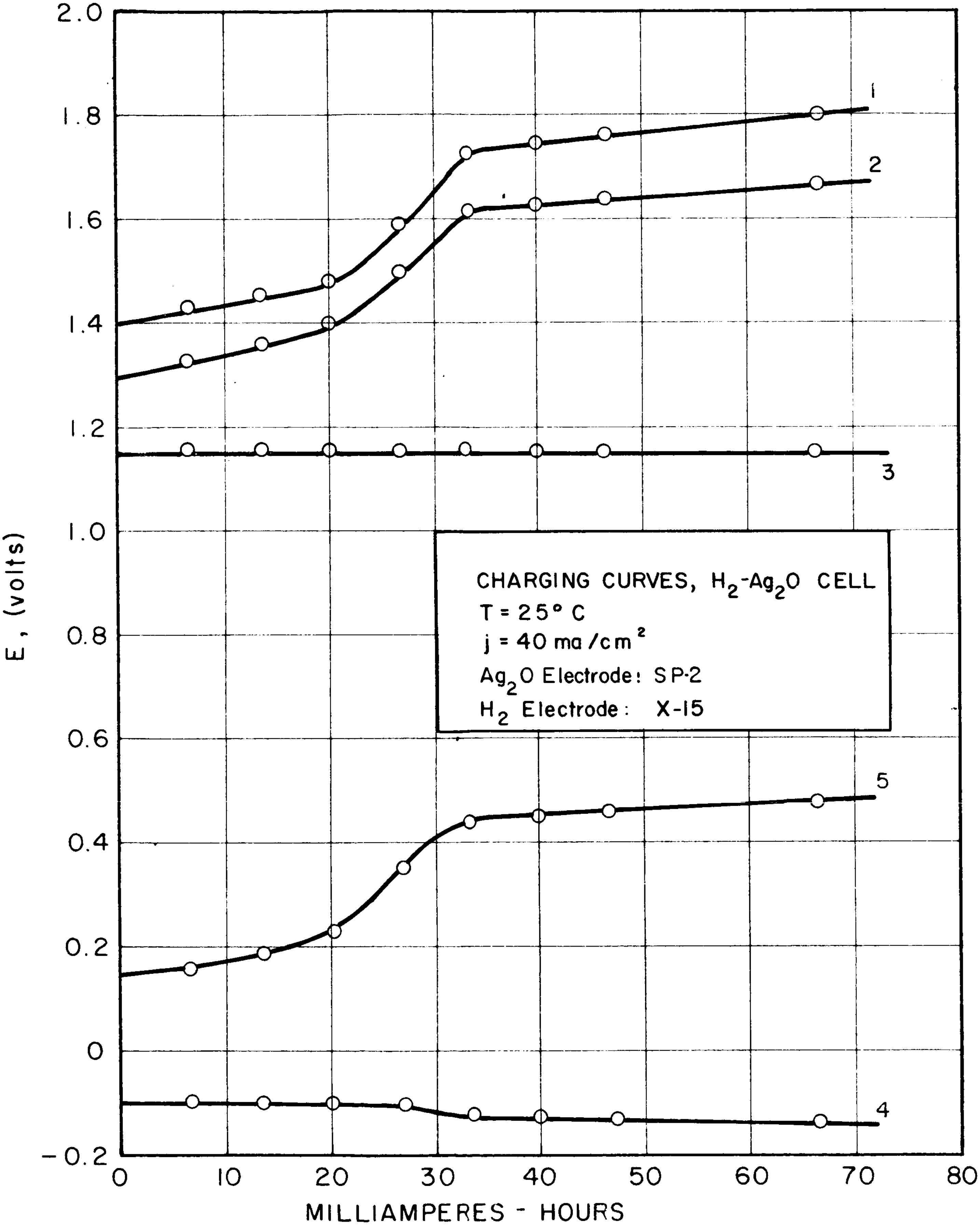

FIG. 20 CHARGING CURVES, HYDROGEN-SILVER OXIDE CELL

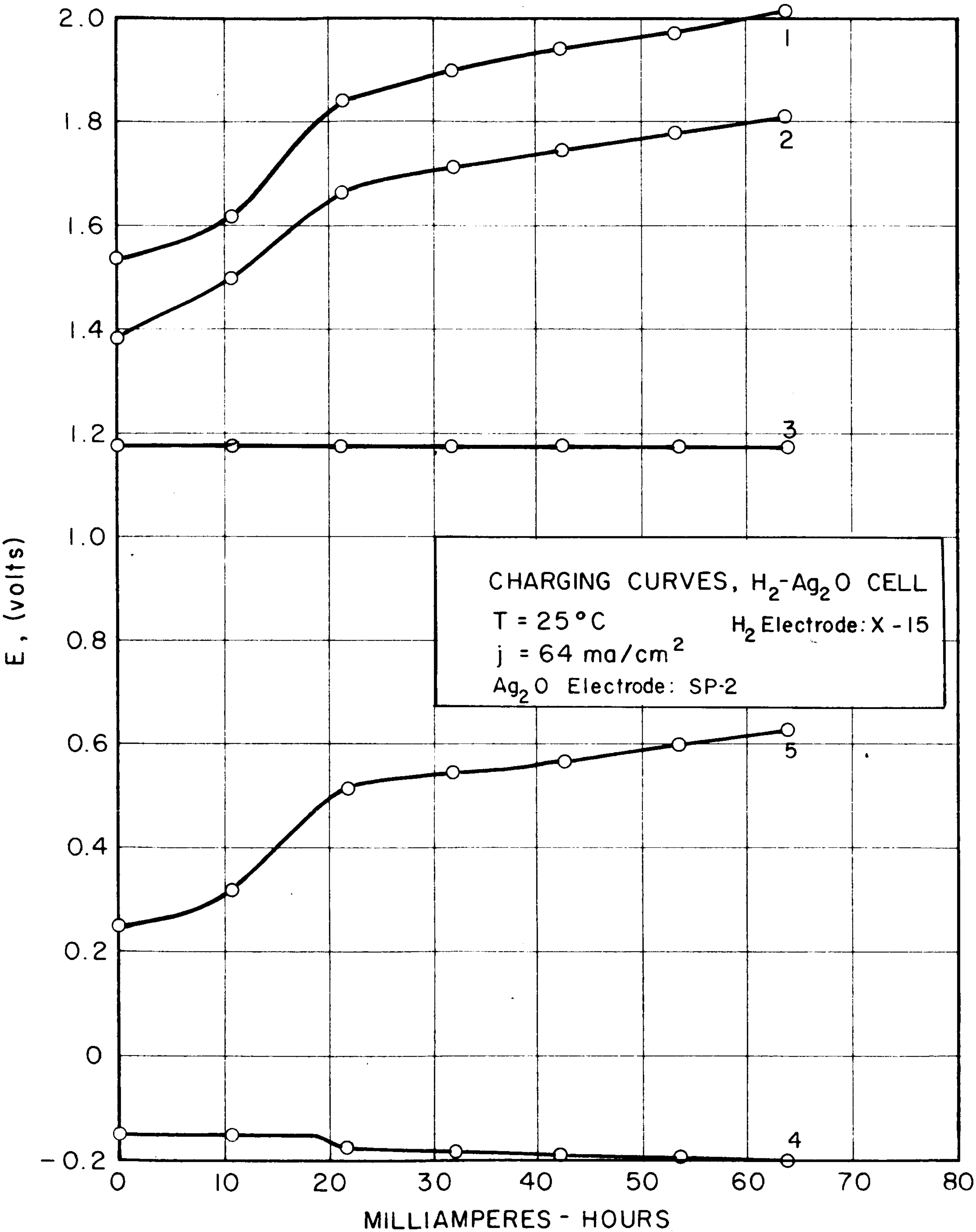

FI . 21 CHARGING C RVES, DROGEN-SILVER OXIDE CELL that channel No. 3 fell and No. 5 did not, and that No. 4 showed a potential of up to a volt or more. Under these circumstances, it was evident that the hydrogen electrode was badly polarized. This was probably the result of flooding, and could nearly always be eliminated by flushing the hydrogen side with hydrogen for a few minutes. However, it was seldom possible to reduce this potential below about 0.01 to 0.02 volt positive, which means the reference was negative with respect to the working electrode. This would cause channel No. 3 to read high, but it was found that it never read high, but low sometimes by as much as 0.03 volt. If it be assumed that the Ag_2O reference electrode was completely unpolarized, then it must be concluded that both hydrogen electrodes were polarized, even on open circuit, and that the reference was polarized 0.01 to 0.02 volt less.

Another observation that could be made is that to within the accuracy of the measuring instruments, the curves were consistent. For example, when the absolute values of No. 4 plus No. 5 are subtracted from No. 3, curve No. 1 results. Also, curve No. 4 is the difference between Nos. 1 and 2. See Table IX.

Each of the above electrodes contained a silver screen which weighed about 1.2 gm. This solid silver screen only partially enters into the reaction, with the result that there is some uncertainty in the reactivity of the material under test. For that reason, all other silver oxide electrodes were made without the screen.

TABLE IX

SILVER ELECTRODE COMPOSITIONS

Electrode	Composition
S-2	Sherical silver (100 - 200 mesh) + asbestos
S-3	Raney silver
S-4	Silpowder No. 130
S-6	75 percent silpowder, 25 percent carbon
SP-1	Precipitated Ag_2O, undoped
SP-7	Precipitated Ag_2O with 0.5 atom percent CoO.

If the oxidation of the screen be assumed negligible, then in ma-hrs/gm, the capacity of the S-3 electrode would be 3.28 times as great as shown in Figure 22 and it would therefore approach the values for those in Figure 23.

In Figure 23 are shown the capacities and polarization characteristics of an undoped silver oxide electrode. The electrode was not analyzed for silver content; however, electrodes of this type usually have about 1.1 to 1.3 gm of silver.

Cobalt doped silver oxide electrodes were compared with undoped silver oxide. The results are shown in Figures 24 and 25. For these experiments, the cells were discharged completely through a 1 ohm resistor and charged until the second silver plateau was reached. The silver electrodes were later analyzed, using the Volhard method, to determine the total amount of silver present.

Since the Ag_2O paste was usually given a final wash with the electrolyte in order to prevent pH gradients, the effect of pH within the electrode was also examined and is shown in Figures 24 and 25. Finally, in Figure 26, the results of a charge at 2.5 ma/cm^2 are shown and compared with those at 40 and 64 ma/cm^2. The electrode material again was cobalt doped. Some experiments with manganese doped silver oxide were performed but they seemed to offer no improvement over the undoped oxide.

5.3 Hydrogen Storage in Palladium

A hydrogen-silver oxide fuel cell would be especially attractive if the hydrogen were stored within the electrode. A hybrid fuel cell would then be obtained, since the hydrogen electrode would be nonconsumable, and in this case, there would be no gas pressure storage.

A hydrogen electrode was fabricated by sintering palladium powder onto a fine platinum screen. A palladium black catalyst was applied by thermally decomposing $PdCl_2$ at $500^{\circ}C$ on the sintered palladium electrode. About 7.5 mg Pd/cm^2 was applied in this manner.

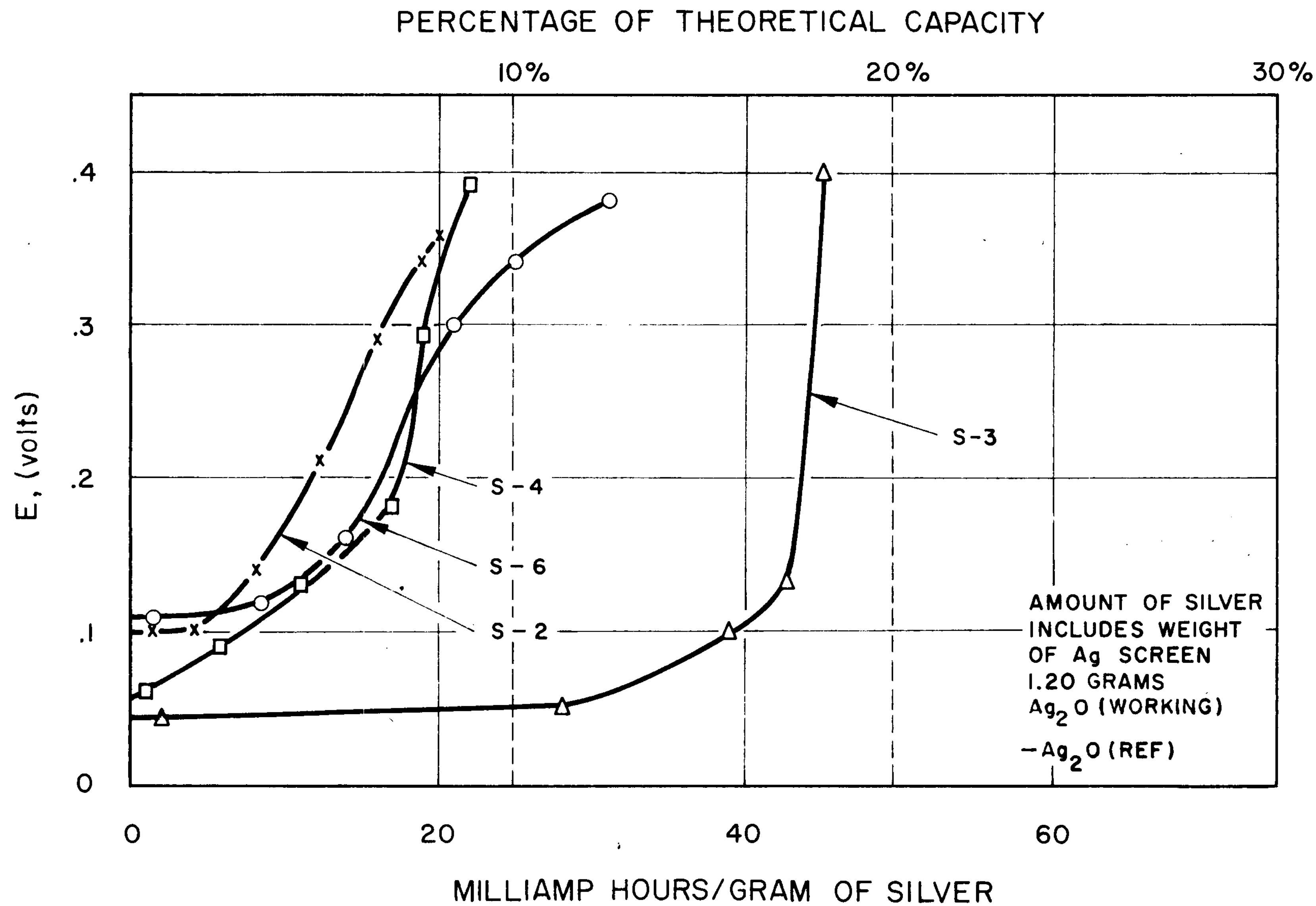

FIG. 22 SILVER ELECTRODE CHARGING CURVES (S-SERIES)

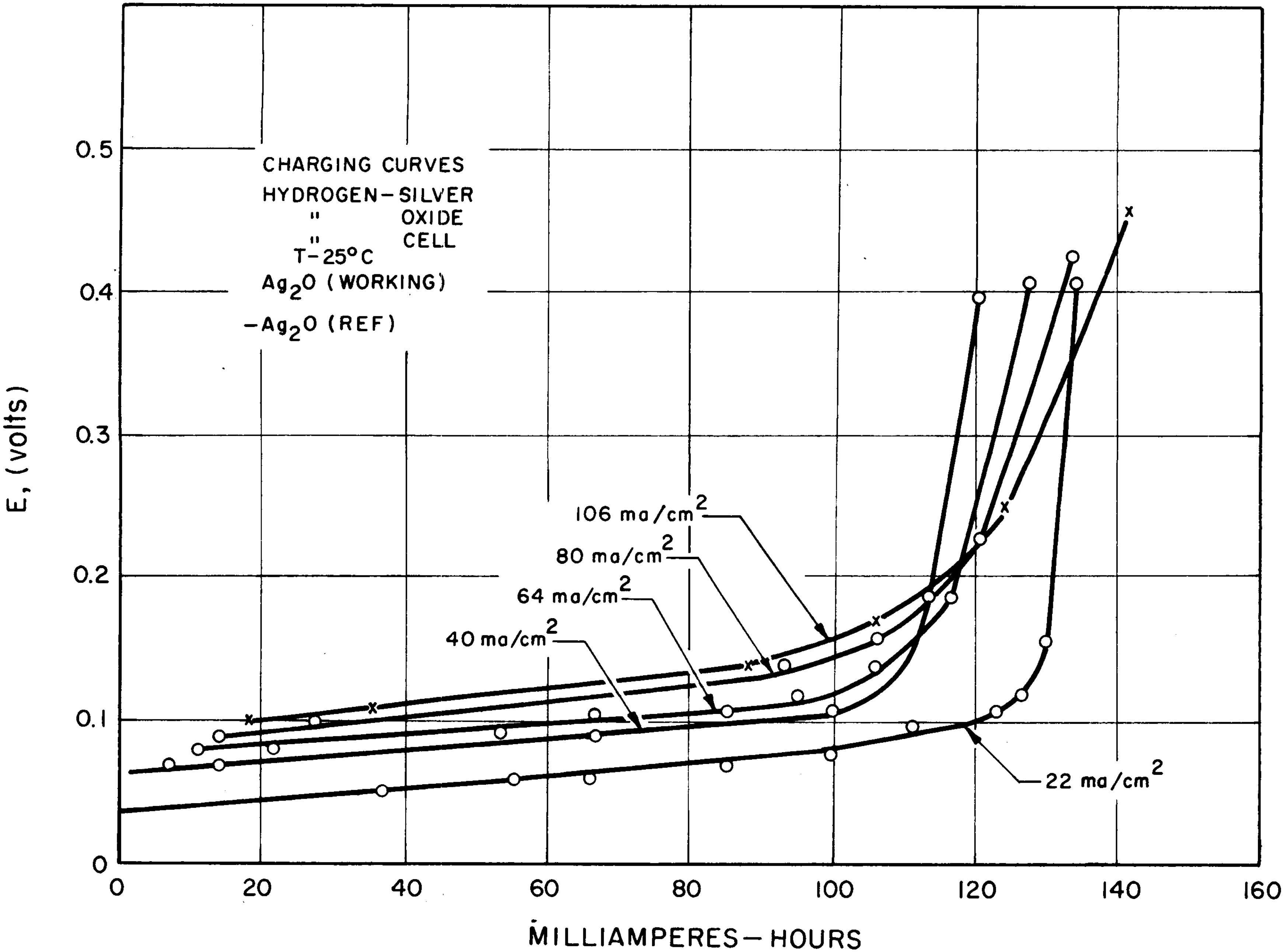

FIG. 23 CHARGING CURVES HYDROGEN-SILVER OXIDE CELL

7367223

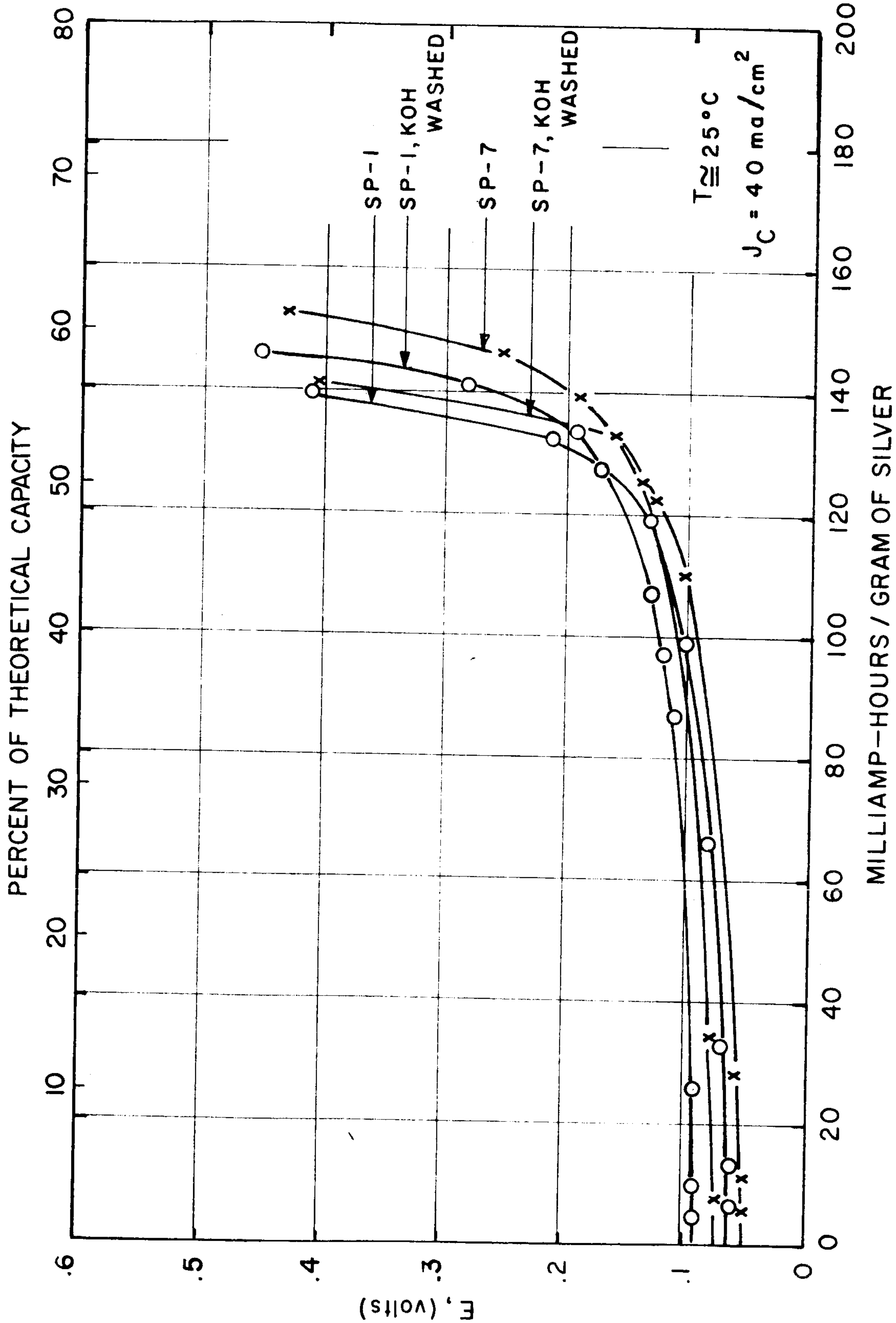

FIG. 24 SILVER ELECTRODE CHARGING CURVES

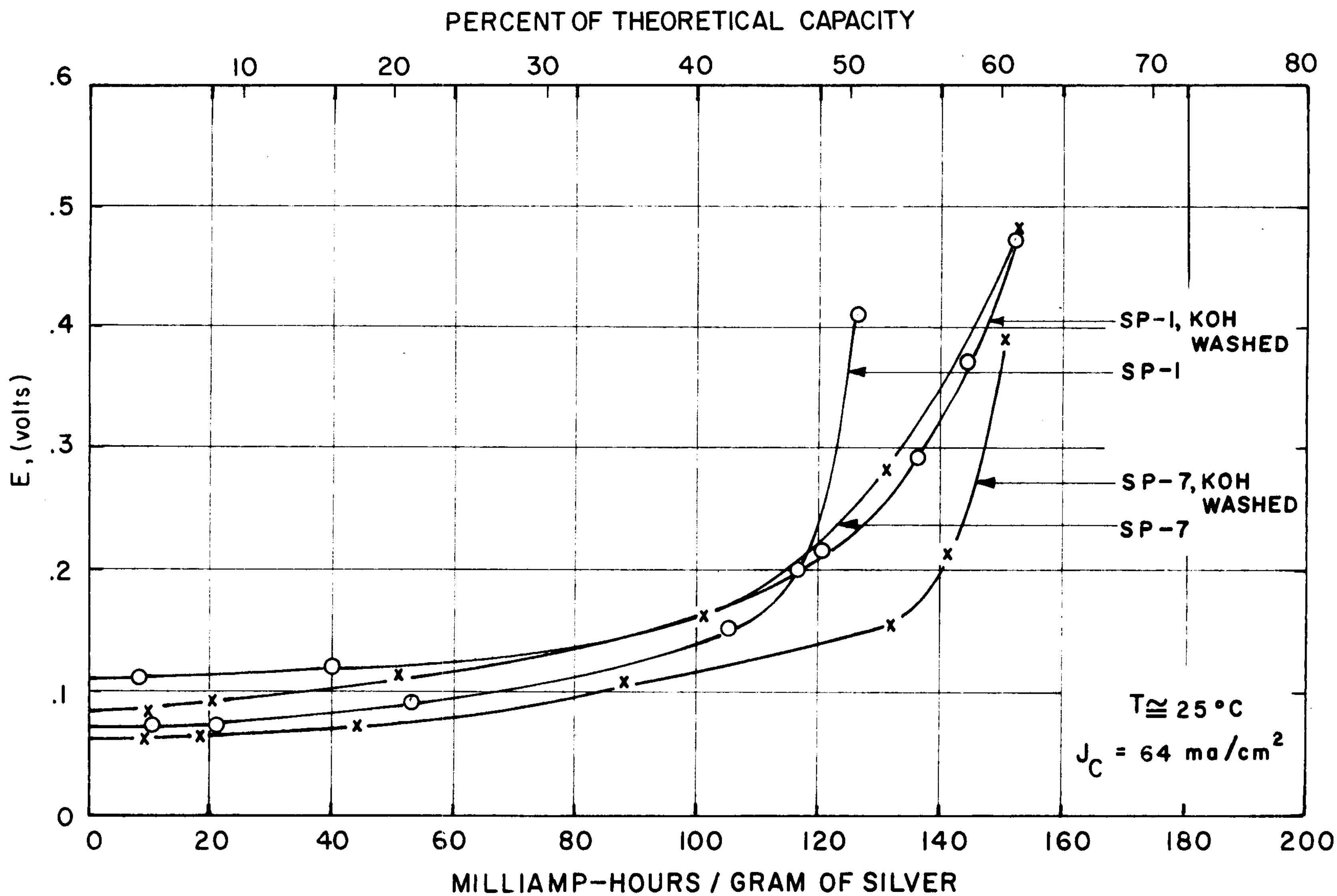

FIG. 25 S.LVER ELECTRODE CHARGING CURVES

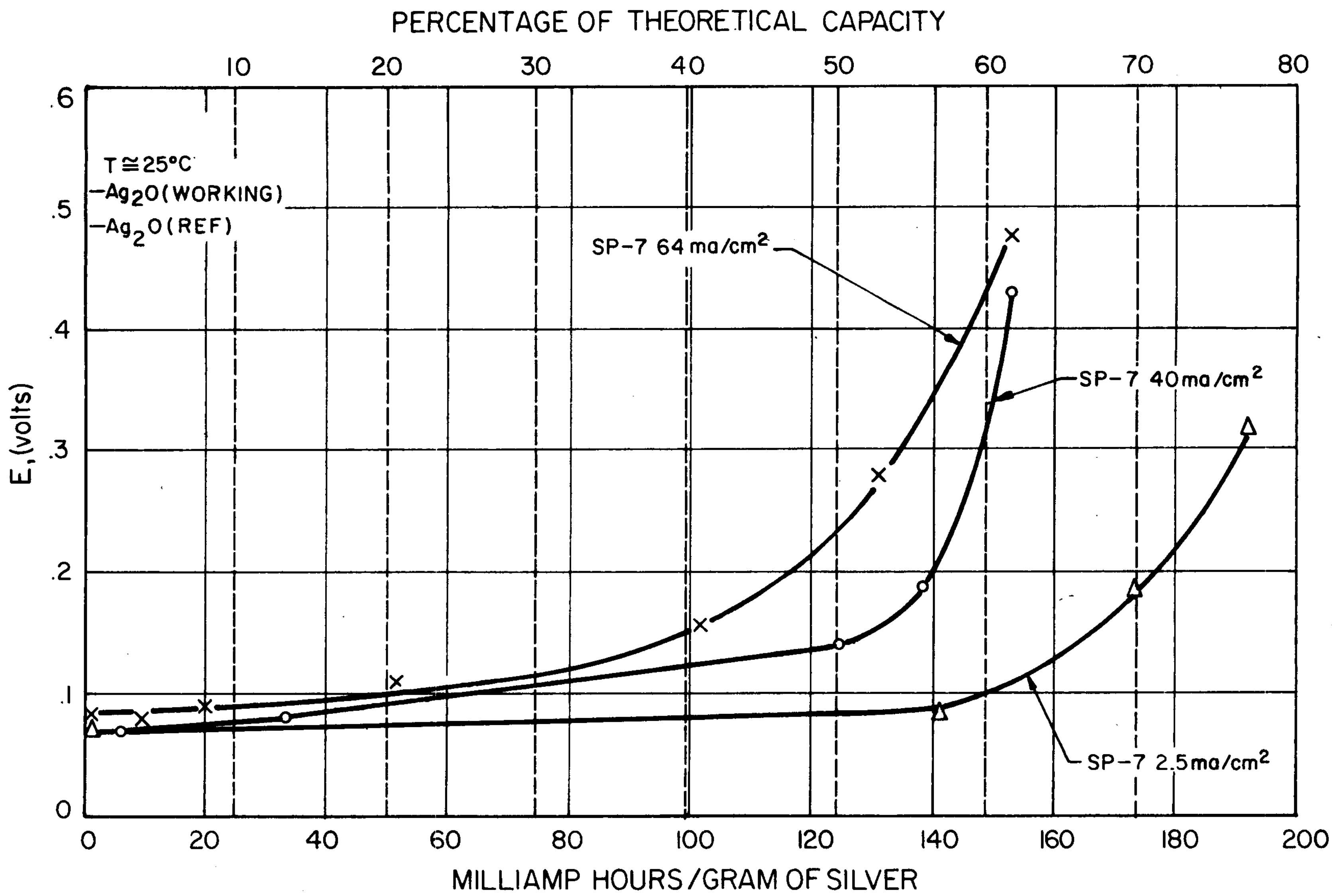

FIG. 26 SILVER ELECTRODE CHARGING CURVES (SP-SERIES)

Pressure was monitored continuously while a hydrogen-silver oxide cell was charged along the first silver plateau, using the sintered palladium for the hydrogen electrode. The object was to determine polarization characteristics and the rate of pressure build-up within the cell.

The results, shown in Figure 27, were generally very satisfactory. It can be seen that there was a very slight increase with time for the three highest charging rates, and the gage pressure was always negative except for the 155 ma/cm^2 rate. At the end of the latter charge there was a positive gage pressure of about 3 psi. The reason for the negative pressures is that the hydrogen side of the cell was swept with hydrogen, in the usual manner, before each run and this was then quickly absorbed by the palladium.

The cells were discharged at the same rates at which they had previously been charged. The amp-hr ratio at 40 ma/cm^2 was 95 percent; at 80 it was 87 percent; at 124 it was 75 percent; and at 155 ma/cm^2 the ratio was 67 percent. The number of ma-hours obtained on discharge was 180, 226, 258, and 104 respectively. The weight of palladium (minus the platinum screen) was 1.399 gm. However, it was not shown that these figures represented the capacity of the palladium or the capacity of the silver.

Polarization characteristics were about normal for a hydrogen electrode catalyzed with pure palladium. No reliable results were obtained for individual electrodes as the hydrogen reference electrode failed repeatedly, probably because it was a platinum catalyzed, sintered nickel electrode and a hydrogen gas pressure could not be maintained on it in the presence of the sintered palladium electrode.

5.4 Hydrogen Storage in Raney Nickel

Raney nickel electrodes were examined very briefly from the standpoint of hydrogen storage in a silver oxide-hydrogen cell. The Raney nickel was made from a 50-50 nickel-aluminum alloy in the form of a powder. After the aluminum was leached out and the material

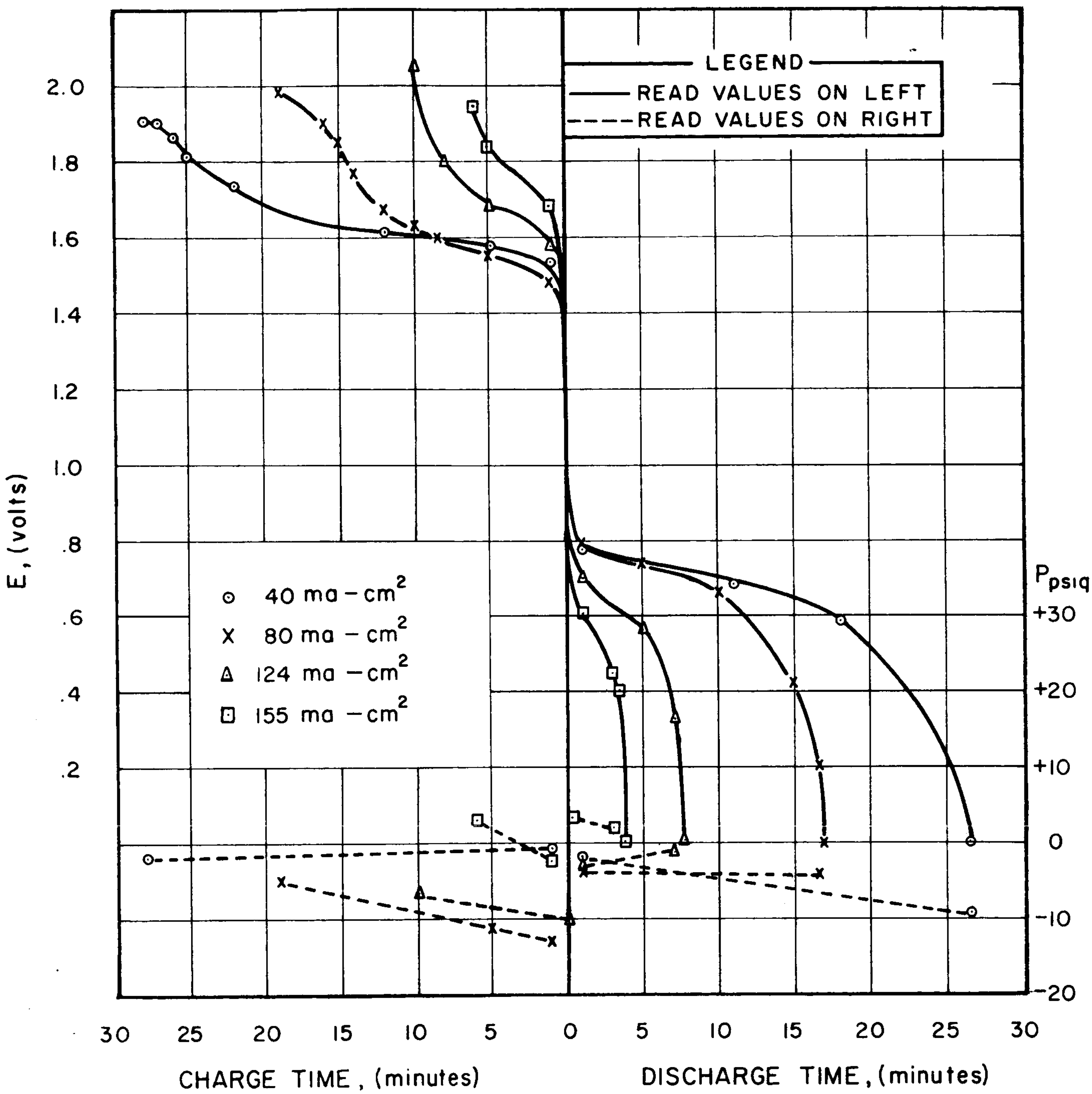

FIG. 27 Ag_2O VS $Pd(H_2)$

washed, an electrode was made by pasting the wet powdered Raney nickel into the electrode space in much the same manner that the silver oxide electrodes were prepared. The Raney nickel powder was fine enough so that it was flooded with electrolyte while in operation. If the Raney nickel absorbs hydrogen in the charging process the way palladium does, then it should not matter that the electrode is flooded, since molecular hydrogen is not formed. Figure 28 shows a constant current charging operation and Figure 29 shows a charge polarization curve. Discharge characteristics were so poor that no similar discharge curves could be obtained.

The most likely explanation for the results is that the Raney nickel electrode was behaving as a gas electrode, in contrast to the palladium electrode. This should not be surprising, however, since hydrogen in true solution in (or combination with) nickel is orders of magnitude less than it is in palladium (Ref. 9). If large amounts of hydrogen can be stored in Raney nickel, then the storage must represent an adsorption process, and the electrode mechanism would not be expected to be like that on palladium.

5.5 Technical Evaluation of Hydrogen-Silver Oxide Fuel Cell Battery

Based on that part of the program that was concerned with the hydrogen-silver oxide fuel cell concept, it seems rather certain that a fuel cell battery based on this system would offer only marginal advantages at best over existing batteries in terms of the energy/weight ratio. Hydrogen storage in palladium is certainly feasible from the standpoint of the ability of palladium to readily take up hydrogen during charge and yield on discharge. The fundamental limitation imposed on the energy/weight ratio is due to the fact that palladium saturated with hydrogen (which can be represented approximately by the formula $PdH_{0.6}$) has an equivalent weight of $\frac{106.4 + 0.6}{0.6}$ or 178.5. This compares for exampke, to 32.7 for zinc and 56.2 for cadmium. When added to the equivalent weight of AgO, which is 61.9, the equivalent weight for the combinations become:

$AgO - PdH_{0.6}$	240.4
$AgO - Cd$	118.1
$AgO - Zn$	94.6

The $AgO-PdH_{0.6}$ system also suffers from a somewhat lower operating voltage than the other two. However, it can be seen from Fig. 27 that a very high fraction of the theoretical hydrogen storage can be realized. As pointed out in Section 5.3, 95 percent current efficiency can be obtained at a charge and discharge current density of 40 ma/cm^2, even when the material was charged to its theoretical capacity.

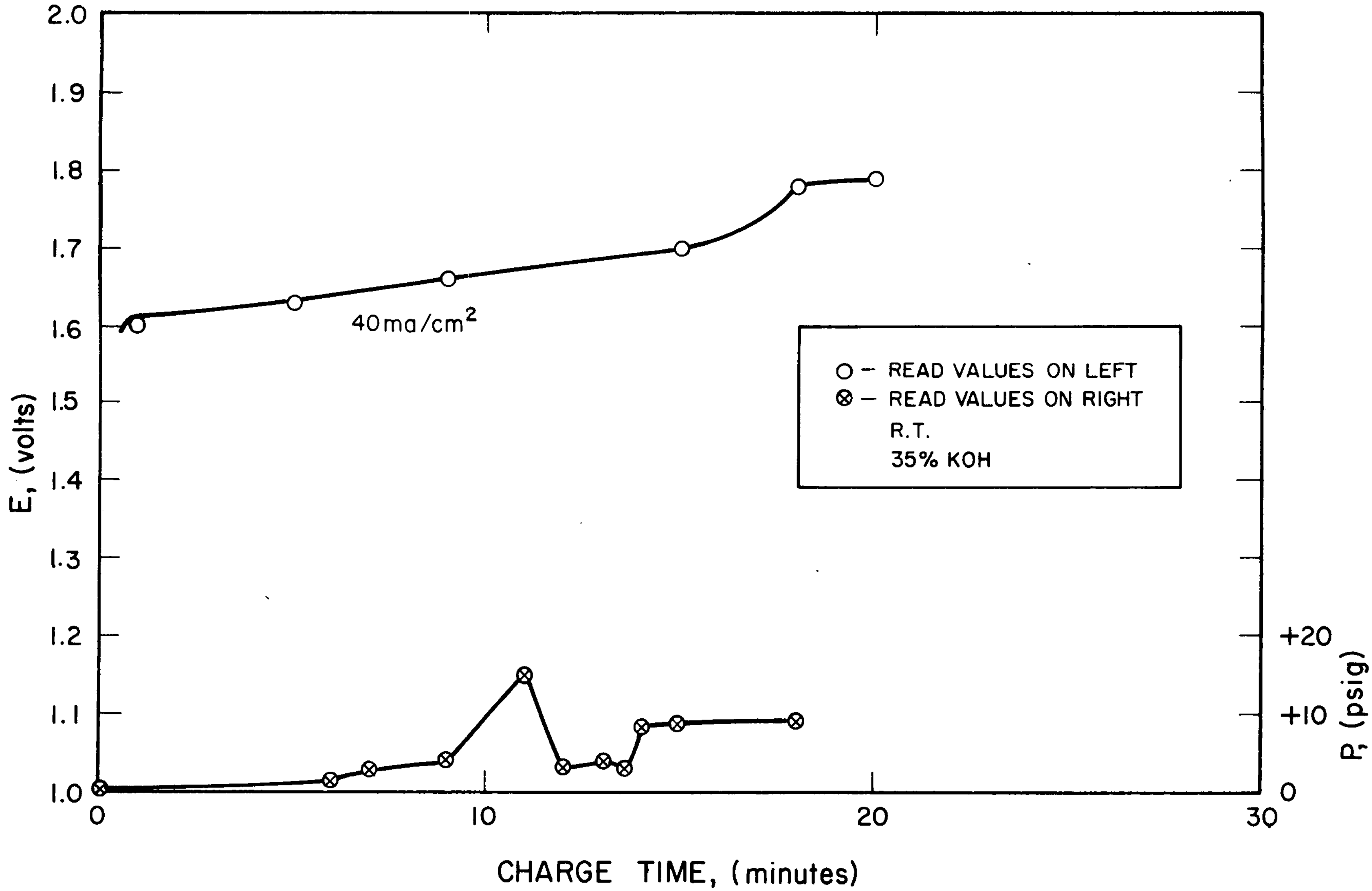

FIG. 28 CHARGE CHARACTERISTICS OF HYDROGEN ON RANEY NICKEL

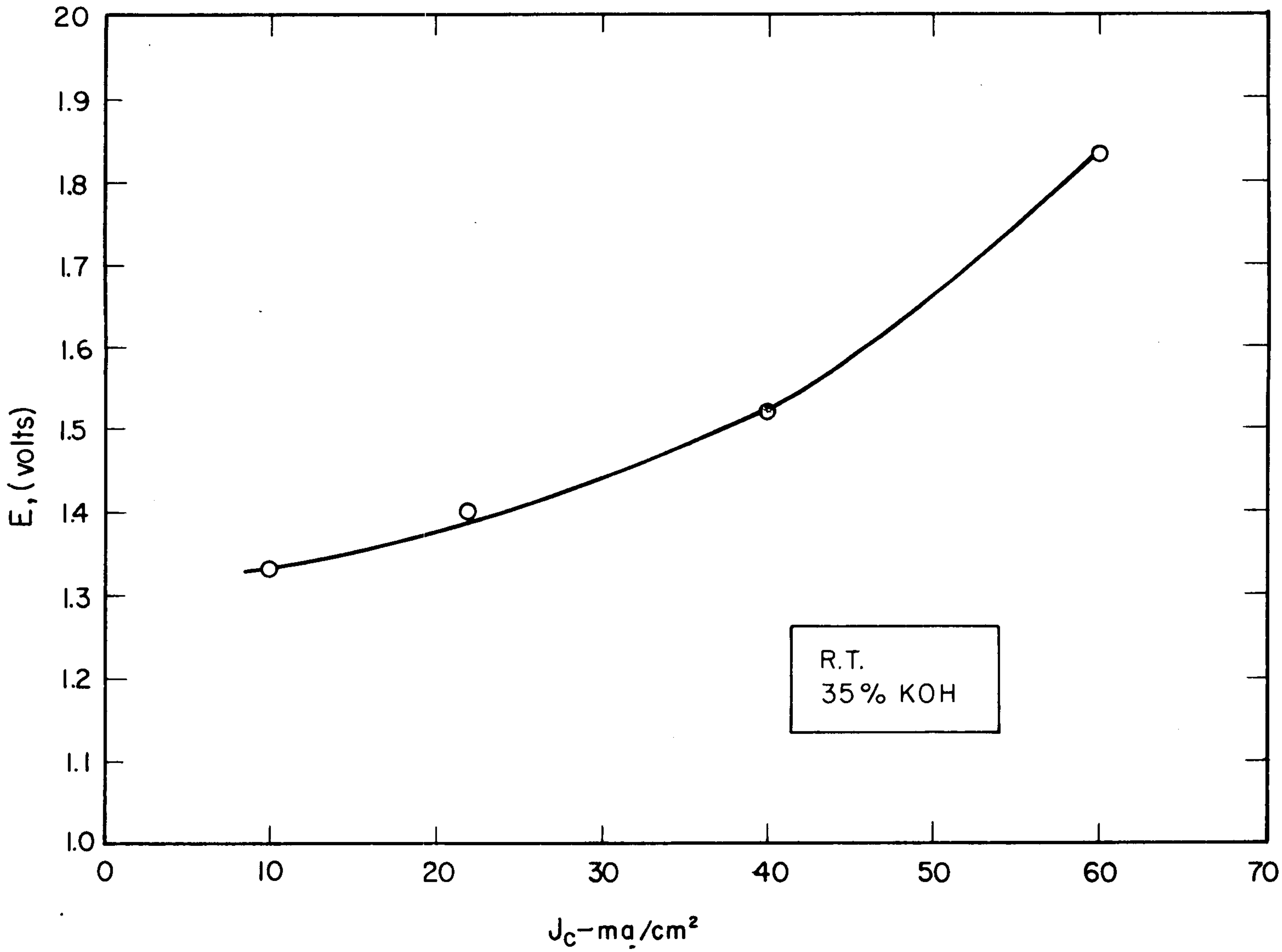

FIG. 29 CHARGE POLARIZATION OF HYDROGEN ON RANEY NICKEL

6. CONCLUSIONS

Considerable progress towards reaching the stated objectives of this program were realized. In particular, the efficiencies, power densities, and capacities of both the hydrogen-silver oxide cell and the hydrogen-oxygen cell were very substantially improved over the corresponding characteristics at the beginning of the program. The general conclusions regarding each cell separately can now be summarized:

6.1 Hydrogen-Silver Oxide Cells

Research concerned with the hydrogen-silver oxide cell yielded the following results:

1. Silver oxide doped with MnO, and especially with CoO, displayed resistivities much lower than that of pure Ag_2O.
2. Electrodes made with the cobalt doped oxide demonstrated much less polarization at a given current density than silver oxide electrodes from commerical batteries (Ref. 10).
3. The same electrodes yielded much greater charging capacity along the first charging plateau than previous commerical silver oxide electrodes (Ref. 10). To the point where the second plateau was reached, capacities up to 77 percent of theoretical were realized, compared to 20 to 40 percent for previously reported silver electrodes (Ref. 8).

4. The same electrodes displayed an absence of the voltage peak ordinarily associated with silver electrodes as the charging changes from the first to the second plateau. This characteristic of these electrodes is significant in systems with voltage regulators which stop the charging of the cell at a preset voltage, in order to prevent gassing.
5. The feasibility of storing hydrogen within a palladium electrode, thereby producing a hydrogen-silver oxide cell with no pressure storage, was demonstrated. However, this system would seem to offer no advantage in energy/weight ratio over some existing systems.

6.2 Hydrogen-Oxygen Cells

Research concerned with the hydrogen-oxygen cell yielded the following results:

1. An improved catalyst plating procedure for nickel electrodes was developed.
2. The effects of both total and differential pressures on each electrode were determined.
3. Temperature dependence on electrode polarization was established.
4. The effect of mixed platinum-palladium catalysts was studied and the optimum ratio of the two catalysts was determined.
5. The effects of electrolyte impurities were studied.
6. Evaluation of Pm^{147} and Po^{210} doped silver electrodes for the cathode in hydrogen-oxygen cells was made. However, our results showed no correlation with radioactivity.

7. The effect of electrolyte concentration on electrode polarization was studied. These studies were especially pertinent to rechargeable cells as this effect establishes, in part, the range of concentration over which these cells can be operated.
8. The feasibility of a method of storing extra electrolyte (other than between the electrodes) within a cell was demonstrated. The importance of this is that cell capacity is determined by the amount of useable water in the system.
9. Gas diffusion rates through the electrolyte bed were established and possibilities for decreasing these rates were suggested.

As the result of the electrode studies outlined above, a very significant improvement in cell performance was accomplished during the course of the program. Power densities up to 90 mw/cm^2 at room temperature were demonstrated. About 150 mw/cm^2 was attained at $70^{\circ}C$. Figure 30 shows a charge-discharge curve at room temperature and a discharge curve at $70^{\circ}C$.

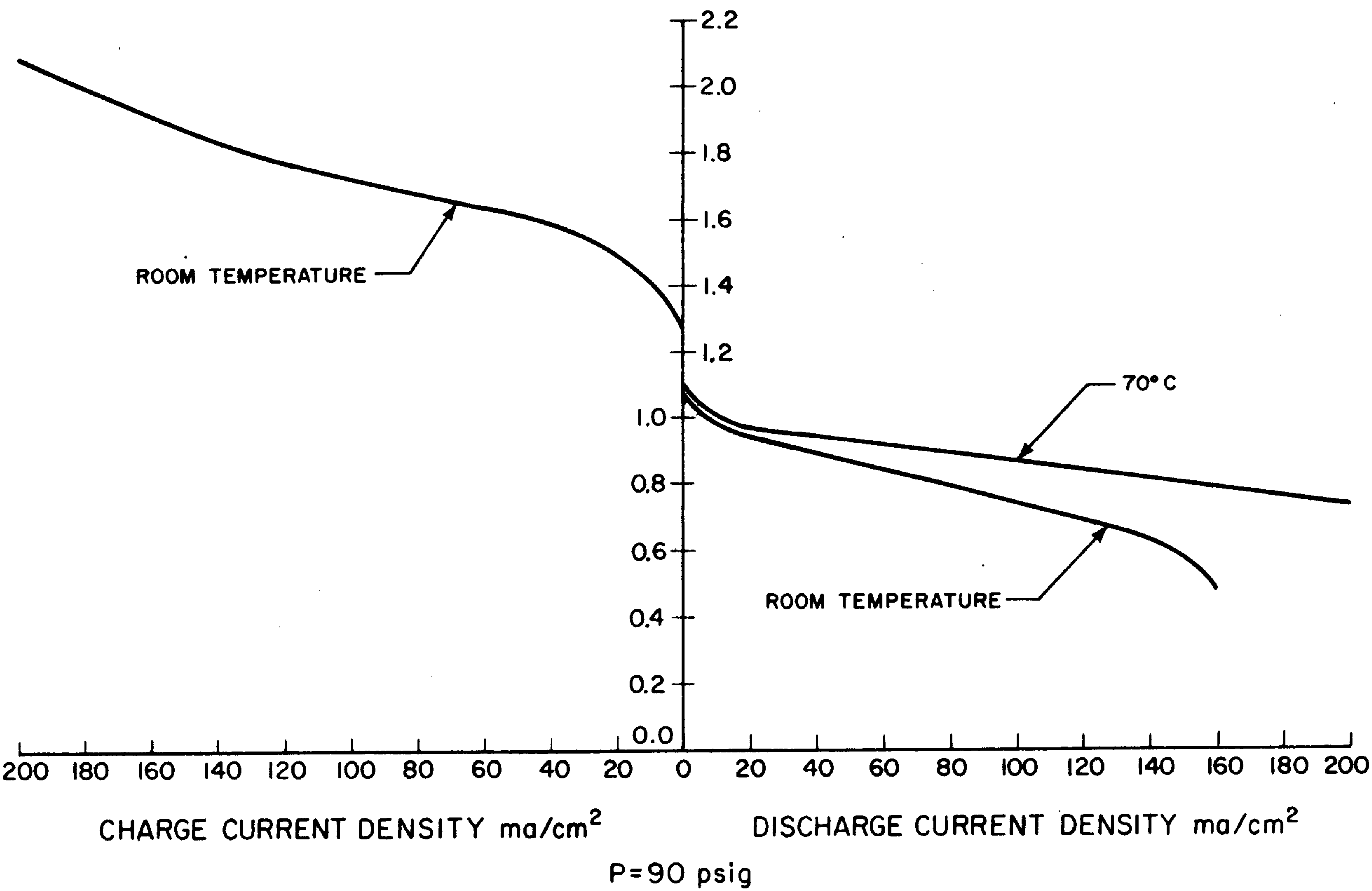

FIG. 30 A CHARGE-DISCHARGE CURVE AT ROOM TEMPERATURE AND A DISCHARGE CURVE AT 70°C

REFERENCES

1. E. A. Oster, "Ion Exchange Fuel Cell Report No. 1", General Electric Company, Lynn, Massachusetts, for Contract No. DA-36-039-SC-89140, 31 December 1961.

2. F. Feigl, "Spot Tests", Vol. I., "Inorganic Applications", pp. 129-30, Elsevier Publishing Company, New York.

3. W. M. Latimer, "Oxidation Potentials", Second Edition, Prentice-Hall, Inc.

4. R. E. Smith, E. T. Friess, and M. F. Morales, J. Phys. Chem. 59, 382-3 (1955).

5. G. Tamann and V. Jessen, Z. Amorg. Allgem. Chem. 179, 125-44 (1929).

6. H. W. Rotthauwe, Kiel. Meeresforsch, 14, 48-63 (1958).

7. T. Dirkse, J. Electrochem. Soc., 106, 453-7 (1959).

8. T. Dirkse, J. Electrochem. Soc., 106, 920-5 (1959).

9. Therald Moeller, "Inorganic Chemistry", John Wiley and Sons, Inc., p 412, 1952.

10. C. P. Wales, "The Silver-Silver Oxide Electrode", Part 1, "Anodic Oxidation in Alkaline Solutions", U. S. Naval Research Laboratory, Washington, D. C., November 3, 1960.